Origin and fate of long-chain polyunsaturated fatty acids in the Kerguelen Islands region (Southern Ocean) in late summer

Marine Remize, Frédéric Planchon, Ai Ning Loh, Fabienne Le Grand, Antoine Bideau, Eleonora Puccinelli, Aswani Volety, Philippe Soudant

Origin and fate of long-chain polyunsaturated fatty acids in the Kerguelen Islands region (Southern Ocean) in late summer

Marine REMIZE[1,2], Frédéric PLANCHON[1,*], Ai Ning LOH[2], Fabienne LE GRAND[1], Antoine BIDEAU[1], Eleonora PUCCINELLI[1], Aswani VOLETY[3], Philippe SOUDANT[1*]

[1] Univ Brest, CNRS, IRD, Ifremer, UMR 6539 LEMAR F-29280 Plouzané, France
[2] University of North Carolina Wilmington, Department of Earth and Ocean Sciences, Center for Marine Science, 5600 Marvin K. Moss Ln, WILMINGTON NC 28403 USA
[3] Elon University, 50 Campus Drive, ELON NC 27244 USA

* Correspondence: frederic.planchon@univ-brest.fr; philippe.soudant@univ-brest.fr

Highlights:

- FA profiles of SPOM from the Kerguelen region during the post-bloom period was dominantly composed of PUFA with high proportions of the two LC-PUFA 20:5n-3 and 22:6n-3.
- Abundance of LC-PUFA in the mixed layer derived from the phytoplankton community composed of small species (prymnesiophytes and prasinophytes) and diatoms.
- In the upper mesopelagic, LC-PUFA are maintained at high proportions according to distinct pathways, export of diatoms for 20:5n-3 and zooplankton fecal material for 22:6n-3.
- SPOM revealed high nutritional quality in the upper water column (0-300m) both in the iron-fertilized area on the Plateau and outside in HNLC waters.

Abstract:

Long-chain polyunsaturated fatty acids (LC-PUFA) are molecules produced at the basis of marine food webs and essential for ecosystem functioning. This study reports detailed fatty acid (FA) composition including the two LC-PUFA 20:5n-3 and 22:6n-3, in suspended organic matter (SPOM) from the upper 300 m collected in the Kerguelen Island region in the Southern Ocean during the post-bloom period (February–March 2018; project MOBYDICK). FA profiles were largely dominated by PUFA (53-69 % of Total Fatty Acid, TFA) regardless of stations and among PUFA, proportions of LC-PUFA were especially high, making up 27-44 % of TFA both in the ML

and upper mesopelagic. 20:5n-3 and 22:6n-3 co-occurred in the ML as a result of the post-bloom phytoplankton community showing a mixed composition dominated by small size phytoplankton (prymnesiophytes and prasinophytes) supplying 22:6n-3, and with diatoms in lower proportions supplying 20:5n-3. Elevated levels of LC-PUFA were observed both inside the iron-fertilized area on the Kerguelen Plateau and downstream, and outside in High Nutrient Low Chlorophyll waters located upstream of the Plateau, and appeared unrelated to site. In the upper mesopelagic, both LC-PUFA were maintained at high relative proportions suggesting an efficient and possibly fast vertical transfer from the surface. Transfer with depth seems to proceed via distinct pathways according to LC-PUFA. 20:5n-3 may be exported along with diatoms, presumably in the form of large intact cells, aggregates as well as resting spores. For 22:6n-3, transfer may involve a channeling through the heterotrophic food web resulting in its association with fecal material at depth. Channeling of 22:6n-3 could involve heterotrophic protists such as dinoflagellates and ciliates grazing on small phytoplankton, as well as larger zooplankton such as copepods and salps, possibly feeding on microzooplankton and producing fecal pellets rich in 22:6n-3. According to LC-PUFA content, SPOM present throughout the upper water column (0-300 m) appeared of high nutritional quality both on- and off-plateau, and represented a valuable source of food for secondary consumers and suspension feeders.

Keywords: Essential fatty acids, vertical distribution, fatty acid export, phytoplankton diversity, diatoms, heterotrophic interactions, nutritional quality.

A. INTRODUCTION

The Southern Ocean (SO) is a vast and contrasted environment where the characteristics of pelagic ecosystems are particularly diverse. The Antarctic Circumpolar Current (ACC) composed of successive hydrographic fronts (Orsi et al., 1995) acts as a strong physical and biogeochemical boundary for biological activity, and to the south and until the Antarctic sea ice, lies the largest High Nutrient Low Chlorophyll (HNLC) zone of the world ocean. The productivity is low throughout the year in HNLC open waters essentially due to a lack of dissolved iron (Blain et al., 2007; de Baar et al., 1995; Martin, 1990), and high concentrations of unused macronutrients (phosphate, nitrate, silicic acid) persist in surface waters. In contrast, high productivity regimes are only found close or downstream of Subantarctic islands (South-Georgia, Crozet, Kerguelen, Heard) and continental shelves, which receive natural and persistent iron inputs (Blain et al., 2008; Perissinotto and Duncombe Rae, 1990; Pollard et al., 2007; van der Merwe et al., 2015; Venables and Moore, 2010). Iron fertilization allows phytoplankton, mainly initially composed of diatoms and also *Phaeocystis*, to thrive during intense and long-lasting blooms in austral spring/summer (Cavagna et al., 2015; Korb and Whitehouse, 2004; Mongin et al., 2008; Schallenberg et al., 2018; Schlosser et al., 2018; Seeyave et al., 2007). These blooms provide abundant food and energy to heterotrophic organisms and higher trophic levels, and help to maintain highly productive food webs extended from microbes to zooplankton, micronekton, up to emblematic top-predators of the SO (marine mammals, sea-birds, penguins, whales) (El-Sayed, 1988; Evans and Brussaard, 2012; Pakhomov and McQuaid, 1996).

In the current context of climate change, major modifications are predicted for the SO such as sea surface warming, increasing stratification and reduction in nutrient supplies, southward migration of oceanographic fronts, shrinking of sea ice, as well as ocean acidification, and it already concerns some areas like the Antarctic peninsula (Constable et al., 2014; Moline et al., 2004). These climate-induced changes are likely to affect phytoplankton distribution and composition (Deppeler and Davidson, 2017), and hence to have positive or negative cascade effects on the whole food web. It is therefore important to determine what parameters control the present-day stability, health and resilience of these pristine ecosystems.

Among the parameters that maintains ecosystem stability, the nutritional value of phytoplankton is crucial, as it determines the amount of energy that can flow through the entire food web and controls its overall functioning. Part of nutritional quality for marine organisms is attributable to lipids, in particular to n-3 long-chain polyunsaturated fatty acids (n-3 LC-PUFA) such as 20:5n-3 (eicosapentaenoic acid, EPA) and 22:6n-3 (docosahexaenoic acid, DHA). n-3 LC-PUFA are molecules essential to all organisms and are involved in a variety of physiological processes such as growth, immunity, cell membrane function regulation and energy storage (Guschina and Harwood, 2006; Parrish, 2013). They play important roles in trophic interactions, starting from secondary consumers such as copepods and other crustacean zooplankton, for which they determine growth potential, reproduction success and general fitness (Brett et al., 2009; Brett and Müller-Navarra, 1997; Müller-Navarra et al., 2000; Pond et al., 2005). LC-PUFA are synthetized at the basis of the food web, essentially by phytoplankton and to some extent by small heterotrophs, and the supplies to consumers occur necessarily through diet (Bec et al., 2006; Guo et al., 2017; Klein-Breteler et al., 1999). The production of LC-PUFA by phytoplankton, and fatty acids (FA) in general, is highly species-specific both at the phylum and class levels (Cañavate, 2019; Jónasdóttir, 2019; Parrish, 2013) and enables their use as valuable biomarkers (Dalsgaard et al., 2003). Another consequence is that marine algae do not all have the same nutritional value, the most valuable algae in terms of LC-PUFA proportions includes Prymnesiophyceae, Pavlovaphyceae, Bacillariophyceae, Dinophyceae, Cryptophyceae, Eustigmatophyceae followed by, Prasinophyceae and Mamiellophyceae (Jónasdóttir, 2019). The lowest contents are found in Chlorophyceae, Trebouxiophyceae and especially in Cyanobacteria, which are devoid of LC-PUFA (Jónasdóttir, 2019).

In the SO, LC-PUFA are presumably supplied by two distinct groups of phytoplankton, diatoms and flagellates, characterized by specific FA profiles. Diatoms produce preferentially 20:5n-3 along with C16 monounsaturated fatty acids (MUFA) 16:1n-7, and C_{16} PUFA 16:3n-4 and 16:4n-1 (Dalsgaard et al., 2003; Parrish, 2013; Volkman et al., 1998), with only small amounts of 22:6n-3 found in centric diatoms (Dunstan et al., 1993). The other essential n-3 LC-PUFA 22:6n-3 together with C18 PUFA 18:5n-3 are produced preferentially by dinoflagellates as well as some Prymnesiophyceae like the coccolithophore *Emiliana huxleyi* (Jónasdóttir, 2019; Okuyama et al.,

1992; Thomson et al., 2004) but this latter group is scarce in the SO, and thus it is not assumed to be a potential producer. Another important Prymnesiophyceae species, *Phaeocystis sp.*, produces low levels of LC-PUFA (Nichols et al., 1991; Skerratt et al., 1995), but it can represent an important part of the autotrophic biomass especially in the early and late phase of the diatom bloom. This general picture of LC-PUFA sources is generally adopted in diet studies and relies on the identification of diagnostic FA in consumers (Atkinson et al., 2006; Ericson et al., 2018; Hellessey et al., 2020). This generalized view is probably oversimplified as it mostly relies on FA signatures obtained from culture and feeding experiments without accounting for field observations. Moreover, it only takes into account a single autotrophic production pathway for LC-PUFA, whereas alternative routes via heterotrophy and upgrading may exist. As an example, interactions among grazers such as copepods and heterotrophic protozoans (dinoflagellates and ciliates) were shown to substantially increase the nutritional quality of *Phaeocystis globosa*, most probably via the production of LC-PUFA by heterotrophic upgrading (Tang et al., 2001).

For the SO, available data on the natural occurrence of LC-PUFA in phytoplankton, as well as in protists in general, remain scarce, and it received a disproportionally low attention in comparison to larger size organisms (Hellessey et al., 2020; Pond et al., 2005). The few available data concern only surface samples obtained from highly productive regions of the marginal ice zone and coastal Antarctic zone (Fahl and Kattner, 1993; Gillan et al., 1981; Hernando et al., 2018; Nichols et al., 1993; Thomson et al., 2004) as well as of the frontal Subantarctic zone of the Indian sector of the SO (Mayzaud et al., 2007, 2002). This clearly limits our understanding of LC-PUFA cycling in both the surface euphotic zone where production takes place, and in the water column where organic matter (OM) and associated LC-PUFA are considered as labile fraction, and could be degraded, transformed, and even transferred to benthic communities (Budge and Parrish, 1998; Rembauville et al., 2018; Wilson et al., 2010). Recent results obtained from five long-term sediment traps deployed in naturally iron-fertilized settings and HNLC waters of the Polar Front (PF) region (South Georgia, Crozet, Kerguelen) indicate large regional and seasonal fluctuations in FA and PUFA composition of sinking OM (Rembauville et al., 2018). Variations are tightly linked to the ecological vectors responsible for the export of OM (e.g., diatom resting spores, phytoplankton aggregates, zooplankton fecal pellets) (Rembauville et al., 2016, 2015a, 2015b). On the Kerguelen

Plateau, LC-PUFA such as 20:5n-3, which is usually associated to diatoms resting spores (mainly *Chaetoceros*), could be transferred at depth towards the sediments (Rembauville et al., 2018).

Among naturally Fe-fertilized regions, the Kerguelen Island area has received considerable interest over recent decades as it is well suited for studying the contrasted properties of pelagic ecosystems found in the SO. The Kerguelen Plateau, which extends to the southeast of the islands, is a large-scale topographic feature with shallow bathymetry (< 700 m) that benefits from enhanced Fe inputs via diapycnal mixing (Blain et al., 2008; Park et al., 2008) and is subjected to a large-scale (45,000 km²) and long-lasting (October to February) diatom bloom (Mongin et al., 2008). Bloom phenology consists of two successive phases (Pellichero et al., 2020) with a first phase occurring in spring and dominated by small size diatoms forming long-chains (*Chaetoceros*, *Pseudo-nitzschia*) (Lasbleiz et al., 2016) and a second phase occurring in summer and dominated by larger size diatoms (*Eucampia*, *Corethron*) (Armand et al., 2008; Blain et al., 2021; Liu et al., 2020). Productivity is also stimulated downstream of the Plateau (according to the West to East ACC circulation) due to lateral advection of Fe-rich waters (Quéroué et al., 2015; Trull et al., 2015; van der Merwe et al., 2015), which promotes a diatom bloom from October to January. This latter bloom is shorter in duration and lower in intensity, and composed of different phytoplankton community composition in comparison to the central Plateau (Armand et al., 2008; Lasbleiz et al., 2016). Upstream of the Plateau, south-west of the Kerguelen Islands, open waters are away from the influence of the Fe fertilized area, productivity is drastically reduced and considered representative of HNLC conditions found in the SO (Rembauville et al., 2017). Phytoplankton biomass stays low throughout the year (climatological Chlorophyll a (Chl-a) < 0.3 $\mu g.L^{-1}$) except during a short time period (~1 month) in December/January (Fiala et al., 1998; Kopczyńska et al., 1998). Under HNLC regime, pico- and nano- communities composed mostly by *Phaeocystis sp.* predominate most of the time, except during summer when microphytoplankton, such as small diatoms (*Fragilariopsis sp.*) and autotrophic dinoflagellates, are more abundant (Armand et al., 2008; Fiala et al., 1998; Kopczyńska et al., 1998; Lasbleiz et al., 2016; Rembauville et al., 2017).

The MOBYDICK project (Marine Ecosystem Biodiversity and Dynamics of Carbon around Kerguelen: an integrated view) was designed to complement the available description of the

Kerguelen region ecosystems and the main objectives were 1) to track carbon from its initial fixation at the surface to its channeling through the food web and its transfer at depth via export, and 2) to perform a detailed description of the diversity at each trophic level. The oceanographic survey was carried out in late summer/early autumn (February-March 2018) corresponding to the demise of the diatom bloom, a period that was not previously investigated by other surveys carried out during the onset (KEOPS2, October-November 2011) and decline (KEOPS1, January-February 2005) of the bloom. In this study, we investigated the distribution of FA, including the essential LC-PUFA 20:5n-3 and 22:6n-3, in suspended organic matter (SPOM) collected in the upper water column. Our aims were to explore the origin and fate of essential LC-PUFA from the surface to the upper mesopelagic zone at sites with contrasted seasonal productivity regimes found on and off the Kerguelen Plateau. Statistical analyses were used to identify the main drivers of FA profile variability. A selection of FA specific to phytoplankton classes and zooplankton activity was used to identify the main producers of LC-PUFA and to explore the impact of heterotrophic interactions in the upper water column. Finally, PUFA contents were used to discuss the nutritional quality of suspended OM and a comparison between iron-fertilized and HNLC conditions was addressed.

B. MATERIAL & METHODS

Studied area

The MOBYDICK survey was conducted in the Kerguelen Islands area in the Indian sector of the SO on board of *R/V Marion Dufresne II* during late-austral summer 2018 from February 18th to March 28th coinciding with the post bloom phase. Four stations (M1, M2, M3, and M4, Figure 1), were selected to represent the contrasted production regimes encountered in the area and defined on a seasonal basis. Station M2 (bottom depth 520 m) is located in the Fe-enriched area on the central Kerguelen Plateau. This station corresponds to the station A3 investigated during KEOPS1 and KEOPS2 programs. Station M1 (bottom depth 2723 m), located downstream of the Plateau, benefits also from enhanced Fe supplies and exhibit a seasonal moderate production regime. Station M3 (bottom depth 1730 m) and M4 (bottom depth 4731 m) are both located upstream of the Plateau and are representative of HNLC conditions. Station M3, previously investigated as

192 part of the KERFIX time series program (1990-1995) (Jeandel et al., 1998), was at the time of
193 sampling north of the PF in the Polar Frontal Zone (PFZ) according to Pauthenet et al. (2018),
194 while the three other stations were permanently south of the PF. During the survey, repeated
195 visits were performed at most stations at around 10-day interval except at station M1, which was
196 visited only once. As shown in Table 1, three visits were performed at station M2 (M2-1, M2-2,
197 and M2-3) and two at stations M3 and M4 (M3-1, M3-3, M4-1, M4-2).

198 **Hydrological and biogeochemical data**

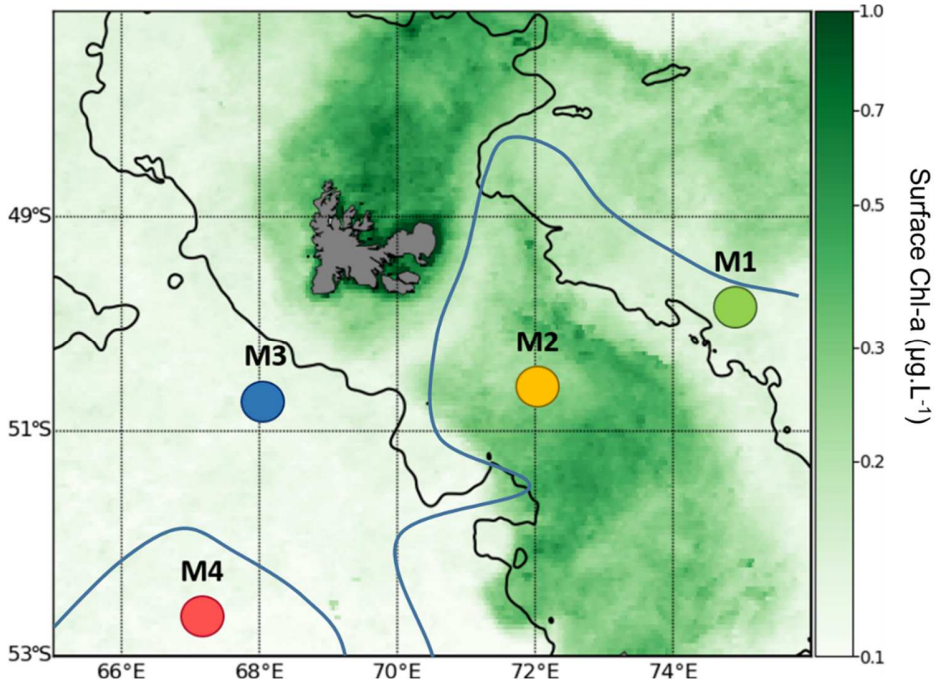

Figure 1 Map of MOBYDICK station locations and monthly mean (March 2018) surface Chlorophyll-a concentrations (µg.L^{-1}) obtained from 4 km resolution Global Ocean Satellite Observations (Copernicus-Globcolour, Copernicus Marine Service, http://marine.copernicus.eu/). The black line refers to 1000 m bathymetry and the blue refers to the approximate position of the PF for the Feb.-Mar. period and drawn according to Pauthenet et al. (2018).

199 Vertical profiles of temperature, dissolved oxygen, and salinity were obtained at all stations
200 using a SeaBird 911-plus CTD (Conductivity, Temperature, and Density) unit mounted on the
201 rosette. Chl-a concentrations and PAR (photosynthetically available radiation) levels were
202 measured using a fluorometer and LI-COR sensor, respectively. The mean depth of the mixed
203 layer (MLD) was estimated based on a difference in potential density of 0.03 to the surface value
204 (10 m) and using all CTD casts performed during the occupation of stations (Lafond et al., 2020).

205 The depth of the euphotic zone (Z_e) corresponded to the depth where light intensity was at least
206 1% of incident light at the surface (Table 1). Averaged Chl-a, silicic acid ($Si(OH)_4$) and ammonium
207 (NH_4^+) concentrations for the mixed layer (ML) are also shown in Table 1, details on the analytical
208 methods can be found elsewhere (Irion et al., 2020; Lafond et al., 2020).

Table 1. MOBYDICK station details, averaged depth of the mixed layer (MLD), depth of the euphotic zone (Ze), and averaged concentrations of Chl-a, silicic acid, ammonium in the mixed layer.

Station	Lat	Lon	Bottom depth	date	Visit	MLD[a]	Ze[b]	Chl-a		$Si(OH)_4$		NH_4	
	°S	°E	m			m	m	µg.L^{-1}		µmol.L^{-1}		µmol.L^{-1}	
								Mean	S.D	Mean	S.D	Mean	S.D
M1	49.9	74.9	2723	10/03/2018	M1	63	89	0.34	0.04	6.7	0.3	0.57	0.21
M2	50.6	72.0	520	27/02/2018	M2-1	79	64	0.27	0.02	1.4	0.4	0.75	0.08
				08/03/2018	M2-2	73	61	0.31	0.05	1.7	0.8	1.12	0.03
				17/03/2018	M2-3	80	58	0.59	0.03	2.8	0.3	0.95	0.06
M3	50.7	68.1	1730	05/03/2018	M3-1	74	93	0.21	0.03	2.9	1.0	0.63	0.22
				19/03/2018	M3-3	96	105	0.14	0.00	2.3	0.2	0.73	0.01
M4	52.6	67.2	4731	03/03/2018	M4-1	69	95	0.19	0.01	4.4	0.4	0.37	0.03
				14/03/2018	M4-2	96	101	0.21	0.01	5.3	1.0	0.54	0.11

[a] MLD: Average mixed layer depth estimated from multiple CTD casts at each station and according to potential density fluctuations < 0.03 kg.m^{-3} relative to 10 m depth.

[b] Ze: Depth of the euphotic zone defined as 1% of surface photosynthetic active radiation.

209

210 **Sampling of suspended particles**

211 Suspended particulate organic matter (SPOM) was sampled for FA determination, at all
212 visited stations (8 stations in total) using five *in situ* pumping systems (ISP) allowing large volume
213 of seawater to be filtered (200-1500 L) and sufficient amount of material to be collected. The five
214 ISP were deployed from the surface euphotic zone to the upper mesopelagic, down to 200 m (M1,
215 M2-2, M2-3, M4-2), 300 m (M2-1, M3-1, M3-3), and 600 m depth (M4-1). For three stations (M1,
216 M2-1, M4-1), only four depths could be sampled due to ISP failures. ISP were equipped for
217 sequential filtration, and we considered here only the 1-50 µm size fraction, which corresponds to
218 the largely dominant fraction in terms of Particulate Organic Carbon (POC, averaged weight
219 proportion 93% of total POC, n=37). For the first six stations (M1, M2-1, M2-2, M4-1, M4-2, M3-1),

the 1-50 μm size fraction was obtained from a single filter made of high-purity quartz microfiber (QMA, Sartorius, France) of 1 μm nominal pore size, and placed after two successive nylon (NITEX) screen pre-filters of 300 and 50 μm mesh size. For the last two stations (M2-3 and M3-3), due to a change in the mesh size of screens (50 and 20 μm), the 1-50 μm fraction was obtained from the QMA filter (1-20 μm) and from the intermediate screen of 20 μm mesh size (20-50 μm).

Samples processing on board

After ISP recovery, the QMA filters were processed on-board as follows: subsampling was conducted directly on the filter using a 25 mm plexiglass punch previously cleaned with ethanol. For FA analyses, four punches were taken and then extracted in 6 mL of 2:1 (v:v) chloroform:methanol solvent and preserved at -20°C. For POC measurements, four other punches were taken, dried at 55°C for 24 hours, and stored at room temperature. For the NITEX screens, the 142 mm filters were cut into quarters using a scalpel (ethanol cleaned), and one quarter was dedicated to POC analyses and another to FA analyses. The two remaining quarters were kept as spare at -20°C. Particles from the NITEX were resuspended using filtered seawater (0.4 μm) and recollected on a pre-combusted 0.7 μm nominal pore-size glass fiber filters (Whatman GF/F, Maidstone, UK). The GF/F filters were processed as described for QMA filters for FA (dived in 6 mL of chloroform:methanol solvent and stored at -20°C) and POC analyses. Lipid extracts dedicated to FA analyses were stored at -20°C during the cruise, shipped to home laboratory (France) with dry ice and stored at -20°C until FA analyses.

Particulate organic carbon analyses

POC samples were fumed with hydrochloric acid (10M) for 4 hours to remove particulate inorganic carbon, dried at ambient temperature for 2 hours, subsampled with a 13 mm punch and encapsulated into tin caps following protocols by Brook et al. (2003) and Trull et al. (2015). POC content was determined using a Flash Elemental Analyzer 2000 coupled to a Thermo Fisher Delta V Plus stable light isotope ratio mass spectrometer system (IRMS, Bremen, Germany). Data were corrected for filter blank contribution, and acetanilide (C_8H_9NO) was used as a standard for POC content. Final concentrations of POC in seawater are reported in $\mu mol.L^{-1}$.

247 **Fatty acids analysis**

248 *a. Lipid extraction and purification*

249 Samples for FA analyses were re-extracted to remove any residual seawater. The initial lipid
250 extract was transferred in a new 22 mL vial, and then re-extracted with 3 mL of chloroform. The
251 sample was vigorously shaken and then centrifuged to insure a good phase separation. For each
252 sample, three re-extractions were performed. Lipid extracts were then evaporated with N_2 gas,
253 resuspended in 6 mL of chloroform:methanol (2:1 v:v) and stored at -20°C until analysis. Lipid
254 extracts were separated into neutral and polar lipids following the method of Remize et al.(2020).
255 Briefly, 3 mL of total lipid extract was evaporated with nitrogen, recovered with three washes
256 using chloroform:methanol (final volume 1.5 mL, 98:2 v:v) and spotted at the top of a silica gel
257 column (40 mm ×4 mm, silica gel 60A 63–200 μm rehydrated with 6% H_2O, 70–230 mesh, Sigma-
258 Aldrich, Darmstadt, Germany). The neutral lipid fraction (NL) was eluted using
259 chloroform:methanol (10 mL 98:2 v:v) and the polar lipid fraction (PL) with methanol (20 mL).
260 Both fractions were then collected in glass vials, and an internal standard (C23:0, 2.3 μg) was
261 added.

262 *b. Transesterification of FAME*

263 Fatty acids methyl esters (FAME) transesterification was conducted according to the protocol
264 described by Mathieu-Resuge et al. (2019). In brief, after evaporation to dryness of the NL and LP
265 fractions, transesterification was performed by adding 0.8 mL of H_2SO_4/methanol mixture (3.4%
266 v:v) to the lipid extract and heated at 100 °C for 10 min. Hexane (0.8 mL) and distilled water
267 saturated with hexane (1.5 mL) were added. The lower MeOH–water phase was discarded after
268 homogenization and centrifugation. Hexane fraction containing FAME was washed two more
269 times with another 1.5 mL of distilled water.

270 *c. Fatty acid analysis by gas chromatography*

271 Analyses of FAME were performed on a Varian CP8400 gas chromatograph (Agilent, Santa Clara
272 CA, USA) using simultaneously two separations on a polar column (ZBWAX: 30 mm × 0.25 mm
273 ID × 0.2 μm, Phenomenex, Torrance, CA, USA) and an apolar column (ZB5HT: 30 m × 0.25 mm

ID × 0.2 µm, Phenomenex, Torrance, CA, USA). The temperature program used by the gas chromatograph was the following: first, initial heating to 0 from 150 °C at 50 °C.min^{-1}, then to 170 °C at 3.5 °C.min^{-1}, to 185 °C at 1.5 °C.min^{-1}, to 225 at 2.4 °C.min^{-1} and finally to 250 °C at 5.5 °C.min^{-1} and maintained for 15 min. The FAME were identified by comparison of their retention time with commercial and in-house standards mixtures as described in Remize et al. (2020).

Table 2. Complete list of FA determined in this study and grouped by compound family with saturated fatty acids (SAFA), monounsaturated fatty acids (MUFA), polyunsaturated fatty acids (PUFA), and branched fatty acids (Branched). Major FA (>1% of TFA of the mean of all samples) are highlighted in bold.

Group	Fatty acids
SAFA	**14:0**, 15:0, **16:0**, 17:0, **18:0**, 20:0, 21:0, 22:0, 24:0
MUFA	14:1n-5, 15:1n-5, 16:1n-9, **16:1n-7**, 16:1n-5, 17:1n-7, **18:1n-9**, **18:1n-7**, 18:1n-5, 20:1n-9, 20:1n-7, 22:1n-9, 22:1n-7, 24:1n-9
PUFA	C_{16}: 16:2n-7, 16:2n-6, 16:2n-4, 16:3n-4, 16:3n-6, 16:3n-3, 16:4n-3, **16:4n-1**
	C_{18}: **18:2n-6**, 18:2n-4, 18:3n-6, 18:3n-4, **18:3n-3**, 18:4n-1, **18:4n-3**, **18:5n-3**
	C_{20}: 20:2n-6**,** 20:3n-6, 20:3n-3, 20:4n-6, 20:4n-3, **20:5n-3**
	C_{21}: 21:5n-3
	C_{22}: 22:2n-6, 22:4n-6, 22:5n-6, 22:5n-3, **22:6n-3**
Branched	iso15:0, ante15:0, iso16:0, iso17:0

FA concentrations reported here correspond to the total lipid fraction (sum of PL and NL fractions) measured in 1-50 µm SPOM. Concentrations are reported in µg.L^{-1} (of seawater) as well as in percent mass proportion relative to total fatty acids (%TFA). The complete list of FA considered and grouped by compound family is shown in Table 2. FA are reported using a shorthand notation of A:Bn-x, where A indicates the number of carbon atoms, B is the number of double bonds and x indicates the position of the first double bond relative to the terminal methyl group (Budge et al., 2006).

Fatty acid profiles in phytoplankton classes

In Table S1, we summarized available information on FA composition of phytoplankton classes provided by the meta-analysis of Jónasdóttir (2019) and Cañavate (2019) as well as the screening study of Mitani et al. (2017). This allows to highlight the relationships between some specific FA abundances and phytoplankton classes.

As seen in Table S1, the percentage of 14:0 is usually above 10% in Mamiellophycea (MAM), Pavlovophycea (PAV), Pelagophycea (PEL), Cosciondiscophycea (COS) and Mediophycea (MED) and above 15% in Coccolithophycea (COC), Prymnesiophycea (PRY), Pinguiophycea (PIN) and Fragilariophycea (FRA). The percentage of 16:1n-7 is above 15% in PAV, Bacillariophyceae (BAC), COS, FRA, and MED. The sum of 16:2n-7, 16:2n-4, 16:3n-4 and 16:4n-1 account for 12% in BAC, 21% in COS, 12% in FRA and 19% in MED while they are only present in trace amounts in other phytoplankton classes. The percentage of 16:4n-3 is above 10% in Chlorophyceae (CHL), Chlorodendrophyceae (CHD), Pyramimonadophyceae (PYR), Prasinophyceae (PRA) and MAM. Percentage of 18:2n-6 is present at 11% in Cyanophyceae (CYA) and 14.5% in Trebouxiophyceae (TRE) while 18:3n-6 is only above 5% in CYA. 18:3n-3 and 18:4n-3 are present in most phytoplankton classes; 18:3n-3 is above 15% in CYA, CHL, TRE, CHD, and Cryptophycea (CRY) while 18:4n-3 is above 12% in PYR, PRA, MAM, CRY PRY, Raphydophyceae (RAP), and PEL. The percentage of 18:5n-3 is especially high in Dinophyceae (DIN) (16%) and present above 5% in PYR, PRA, COC, and PRY. The percentage of 16:4n-3 is above 12% in CHL, CHD, PYR, PRA and MAM, all belonging to the chlorophyta phylum. 20:5n-3 (EPA) ranged between 15% and 20% in PAV, RAP, BAC, COS, FRA, and MED and above 20% in Porphyridophyceae and PIN. 22:6n-3 (DHA) is above 10% in COC, and PRY and above 15% in DIN.

Fatty acids associated to heterotrophic organisms

Branched FA (iso15:0, anteiso15:0, iso16:0 and iso17:0) are associated to bacteria (Parrish, 2013; Volkman et al., 1998; Wilson et al., 2010). The MUFA 20:1n-9, 22:1n-9, 22:1n-7 and 22:1n-11 are specifically produced by zooplankton such as Calanoids (Brett et al., 2009; Dalsgaard et al., 2003; Kattner and Hagen, 1995; Mayzaud et al., 2007; Parrish, 2013; Wilson et al., 2010) and are not found in phytoplankton.

FA-based nutritional quality index

315 FA data were used to estimate the nutritional quality of the 1-50 μm SPOM following the FA-
316 based nutritional quality index (NQI) developed by Cañavate (2019). The NQI was calculated as
317 follow:

318 $$\mathrm{NQI} = [(15 * \mathrm{DHA} + 10 * \mathrm{EPA} + 2 * \mathrm{ARA}) * 0.8 + (1.8 * \sum \mathrm{C18PUFA})] * \log\left(\frac{n-3}{n-6}\right)$$

319 DHA, EPA and 20:4n-6 (arachidonic acid, ARA) are expressed as % of TFA. ΣC18PUFA is the
320 sum of 18:2n-6, 18:3n-3, 18:4n-3 and 18:5n-3 percentages and n-3/n-6 is the ratio of total n-3 PUFA
321 to total n-6 PUFA.

322 **Statistical analysis**

323 Principal Component Analysis (PCA) was used to characterize relationships among FA and
324 to discriminate FA profiles according to depth and station. The PCA was performed with 36 FA
325 out of 55 analyzed whose average abundance was >0.1% of TFA. Resulting components 1, 2 and
326 3 were analyzed using one-way analysis of variance (ANOVA) to identify differences of FA
327 profiles according to depth intervals (ML, MLD-150 m, 150-300 m) and stations. Categories of
328 branched FA, SAFA, MUFA, short-chain PUFA (SC-PUFA), and LC-PUFA were analyzed by non-
329 parametric one-way ANOVA (Krustal-Wallis) with post-hoc analysis to determine significant
330 differences between depth zones (ML, MLD-150 m, 150-300 m). Furthermore, spearman tests were
331 conducted to explore the relationship between some FA and depth. In the surface mixed layer
332 (ML), FA profiles of the 1-50 μm fraction were analyzed by non-parametric one-way ANOVA
333 (Krustal-Wallis) with post-hoc analysis to determine significant differences among stations.
334 Spearman tests were also conducted to explore the relationship between FA profiles and physico-
335 chemical parameters (Temperature, Salinity, Oxygen, NH_4^+, $Si(OH)_4$, NO_3^-) in the ML. Differences
336 were considered statistically significant if $p<0.05$. All statistical analyses were performed using
337 Statgraphics Plus statistical software (Manugistics, Rockville, MD, USA).

338 C. RESULTS

339 **Hydrological and biogeochemical context**

During the first half of the MOBYDICK survey, from late February to early March, the MLD was relatively shallow at all stations (Table 1), varying from 63 m at station M1 to 79 m at station M2-1, and it was consistent with late summer conditions (stable upper water column and low wind stress). After a storm event that occurred on the 10th of March, the MLD deepened consistently at stations M4-2 and M3-3 reaching 96 m, and to a lesser extent on the Plateau at station M2-3 (80 m). The depth of Ze was shallow on the plateau (58-64 m) and above the MLD. Ze was deeper at the other stations (89 m at M1 down to 105 m at M3-3) and it was below the MLD indicating no light limitation in the ML.

In the ML, Chl-a exhibited low values at all stations, with 0.27-0.59 $\mu g.L^{-1}$ and 0.14-0.34 $\mu g.L^{-1}$ on- and off-plateau, respectively. At station M2, Chl-a almost doubled between the second (M2-2) and the third visit (M2-3). Silicic acid had variable concentrations in the ML (Table 1). These were the lowest on the plateau at M2-1 and M2-2 (1.4-1.7 μM), intermediate at M3 (2.3-2.9 μM) and the highest at M4 (4.8 μM) and M1 (6.7 μM). As a comparison, ammonium concentrations, an indicator of heterotrophic excretion, exhibited a reverse trend with highest values on the plateau (0.7-1.1 μM) decreasing to 0.6-0.7 μM at M3 and M1, and were the lowest at M4 (0.3-0.5 μM).

Vertical distribution of TFA concentrations

Depth weighted average (DWA) of TFA concentrations obtained for three depth intervals (ML, MLD-150 m, 150-300 m) are shown in Figure 2. Considering all stations and visits, TFA concentrations were significantly ($p<0.001$) higher in the ML (range: 1.4-3.6 $\mu g.L^{-1}$) as compared to the deeper zones (MLD-150 m and 150-300 m). Although TFA concentrations tended to be lower in the 150-300 m depth interval (range: 0.2-0.7 $\mu g.L^{-1}$) compared to the MLD-150 m zone (range: 0.6-1.6 $\mu g.L^{-1}$), the difference was not significant. TFA concentrations were significantly related to POC ($R^2=0.91$ and $p<0.001$, $n=24$) and therefore to biomass variability. Based on the slope of the regression, the average concentration of TFA in biomass was estimated to be 79±5 $\mu g.mgC^{-1}$.

In the ML, TFA concentrations were not significantly ($p>0.05$) different between on- and off-Plateau stations despite different temporal trends. On the Plateau, TFA concentrations increased from 1.7 to 2.9 $\mu g.L^{-1}$ between stations M2-1 and M2-3. Off the Plateau, TFA concentrations decreased during the course of the survey, from 2.3 to 1.5 $\mu g.L^{-1}$ at station M3 and from 2.4 to 1.4 $\mu g.L^{-1}$ at station M4. The highest TFA concentration in the ML (3.6 $\mu g.L^{-1}$) was found at station M1 downstream of the Plateau. Below the ML, no significant differences ($p>0.05$) were observed according to station locations. On the Plateau, TFA concentration was higher during the first visit of M2-1 (1.6 $\mu g.L^{-1}$) decreasing to 0.6 $\mu g.L^{-1}$ at M2-2, ten days later.

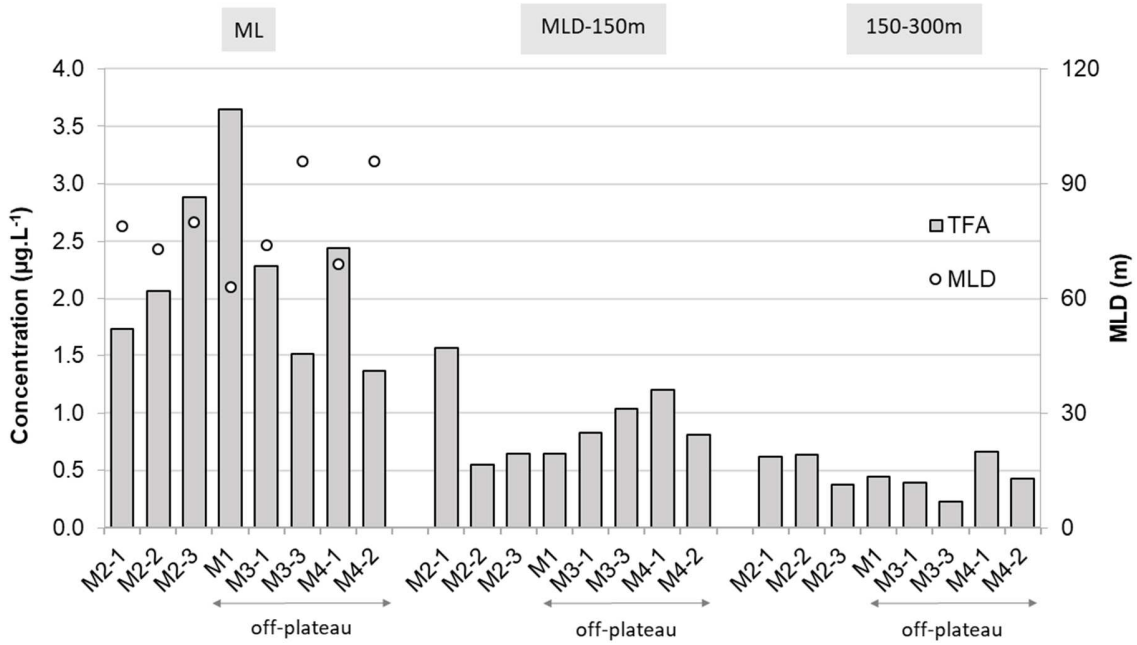

Figure 2: Depth weighted average TFA concentrations (µg.L-1) obtained in three depth intervals (ML, MLD-150m, 150-300m) according the station-visit sampled during the cruise. Also shown, the MLD (m) which was estimated for all stations.

FA partitioning according to unsaturation level

A preliminary partitioning of FA was performed according to the unsaturation level as described in Table 2 and considering branched FA, SAFA, MUFA and PUFA. Within PUFA, we further distinguished SC-PUFA with 16 and 18 atoms of carbon from long-chain PUFA (LC-PUFA) containing 20 and 22 atoms of carbon, which included the essential 20:5n-3 and 22:6n-3.

377 Depth weighted average percentages (relative to TFA) of these five groups are shown in Figure 3.
378 Considering all stations and depths, PUFA were the predominant category (62% on average),

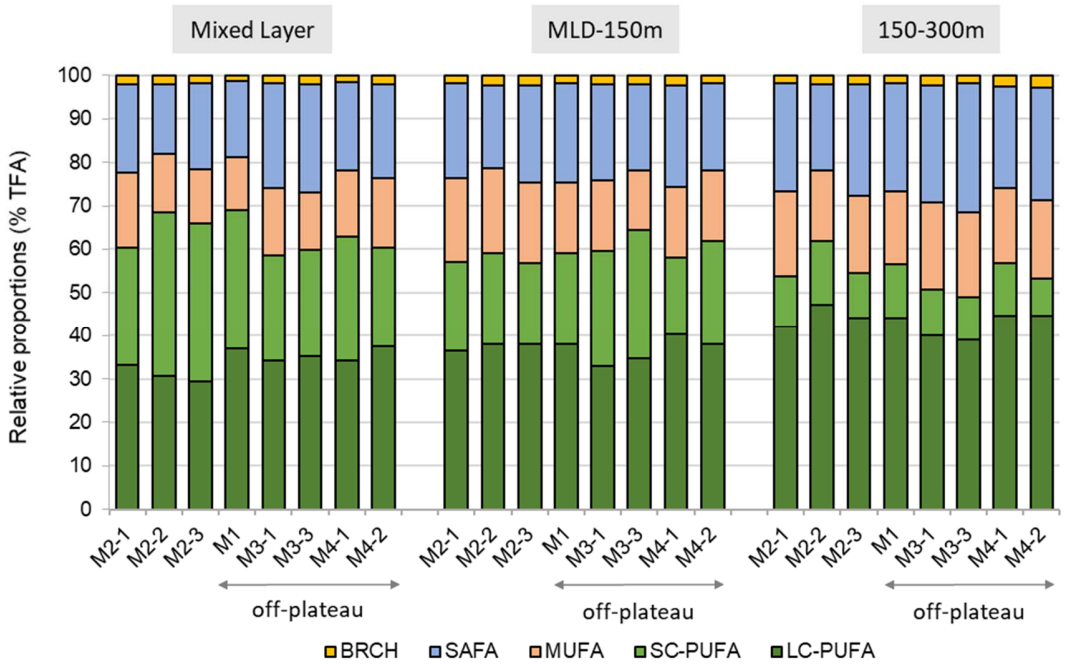

Figure 3: Depth-weighted averaged percentages (relative to TFA) of branched FA (BRCH), saturated FA (SAFA), monounsaturated FA (MUFA), short-chain (C16-C18) and long-chain (C20-C22) polyunsaturated FA (SC-PUFA and LC-PUFA) in three depth intervals (ML, MLD-150, 150-300m).

379 followed by SAFA (21% on average), MUFA (15% on average), and Branched FA (2% on average).
380 Within PUFA, LC-PUFA were dominant (range: 34-44%) and showed increasing and significantly
381 different ($p<0.001$) proportions according to depth interval, 34% in the ML, 37% in the MLD-150
382 m, and 45% in the 150-300 m. On the opposite, SC-PUFA decreased substantially with depth, from
383 30% in the ML down to 12% in the 150-300 m depth interval, and differences between all depth
384 intervals were significant ($p<0.001$). For SAFA and MUFA, proportions increased with depth.
385 Differences were significant ($p<0.01$) only in the 150-300 m compared to the ML and MLD-150 m
386 for SAFA, and in the ML compared to the MLD-150 m and 150-300 m for MUFA.

387 In the ML, no significant differences were observed for SAFA, MUFA, and Branched between
388 on- and off-plateau. LC-PUFA tended to be higher off-plateau compared to on-plateau while SC-
389 PUFA tended to be higher on the plateau vs off-plateau. Below the ML, no significant differences

were observed among stations. However, the decrease of SC-PUFA with depth was faster on the plateau (from 34 to 20%) as compared to off-plateau (from 28 to 24%).

LC-PUFA were dominated by 20:5n-3 and 22:6n-3, both increasing significantly with depth from 13% to 19% for 20:5n-3 and from 18% to 20% for 22:6n-3. SC-PUFA decreased significantly with depth due to the decreases of 18:3n-3, 18:4n-3 and 18:5n-3. In contrast, C16 PUFA associated to diatoms were significantly higher in deep zones (MLD-150m and 150m-300m divisions) than in the ML.

Overall pattern in individual FA abundance

Principal component analysis was applied to 36 FA relative abundances (expressed as % of TFA) by examining 37 cases including FA compositions from 8 stations at various depths and visits. As shown in Figure 4, axis 1 and 2 explained 34.1% and 17.1% of the variability, respectively, and axis 3 12.3% (not shown in Fig. 4). These three axis accounted for >63% of total variability. The positive side of axis 1 was driven by 15:0, 16:0, 18:1n-7, 20:1n-9, 22:1n-9, and 22:1n-7 while 17:1n-7, 18:2n-6, 18:3n-6, 18:3n-3, 18:4n-3 and 18:5n-3 were correlated with the negative side of axis 1. The second axis of the PCA was positively associated to diatom markers including 16:2n-7, 16:2n-4, 16:3n-4, 16:4n-1 and 20:5n-3 and negatively associated to 18:1n-9. The third axis was positively correlated to 16:4n-3. All correlations previously listed (positive or negative) between FA variables and principal components 1, 2, and 3 were highly significant and had correlation coefficients greater than 0.7. As PC1, PC2, and PC3 revealed good correlations (positive and negative) between FA variables, non-parametric analyses of variance with PC1, PC2, and PC3 as the dependent variables and depth intervals and stations as the independent variables were performed. The analysis showed that differences in FA profiles attributable to depth were highly significant (Figure 5) for both PC1 and 2 with p values <0.001 in both cases. While PC1 value increased steadily with depth zones, PC2 value of the MLD-150 m was higher than in the ML and 150-300m zones. While PC1 and PC2 were not significantly different according to stations, PC3 allowed significant differentiation between on-plateau station M2 and off-plateau stations M3 and M4 ($p<0.01$, Figure 5).

418

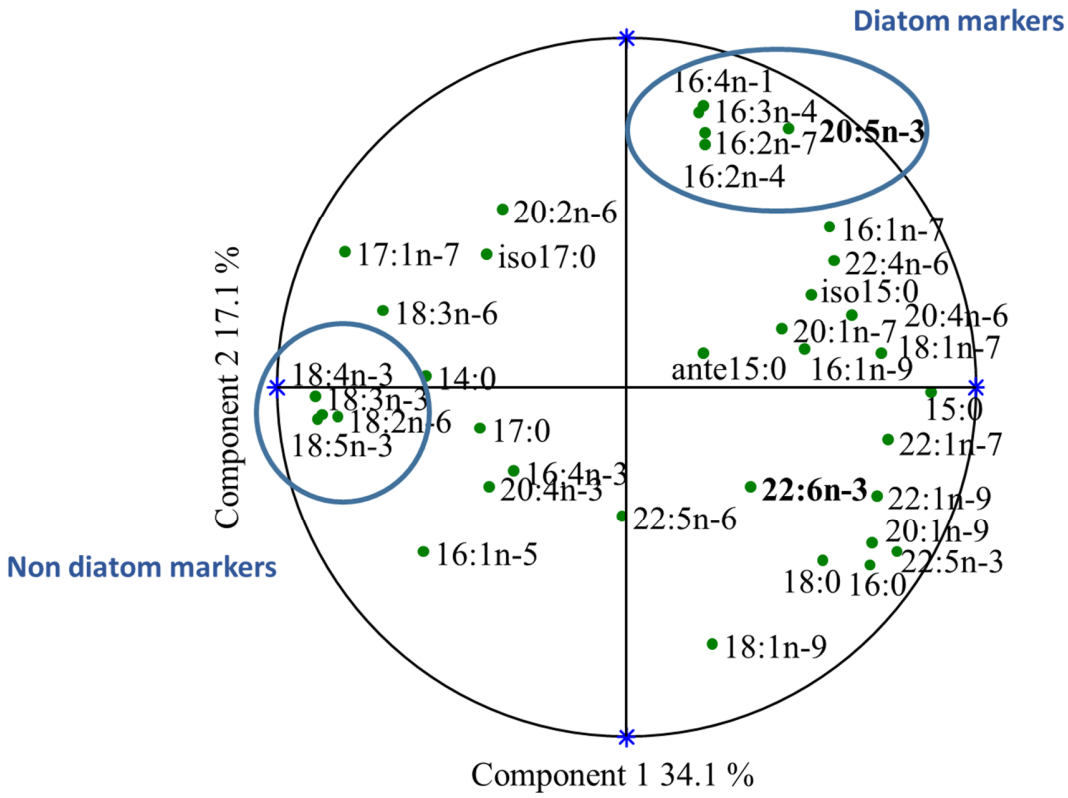

Figure 4: Correlation circle of 36 fatty acid variables according to the two principal components 1 and 2 obtained from the Principal Component Analysis, which used 37 cases including FA compositions of 1-50 µm suspended particulate organic matter from 8 stations at various depths. The outer circle represents the unit circle in terms of correlation coefficient (positive or negative along each axis). The closer the FA variables are to the outer circle, the higher the correlation coefficient.

419

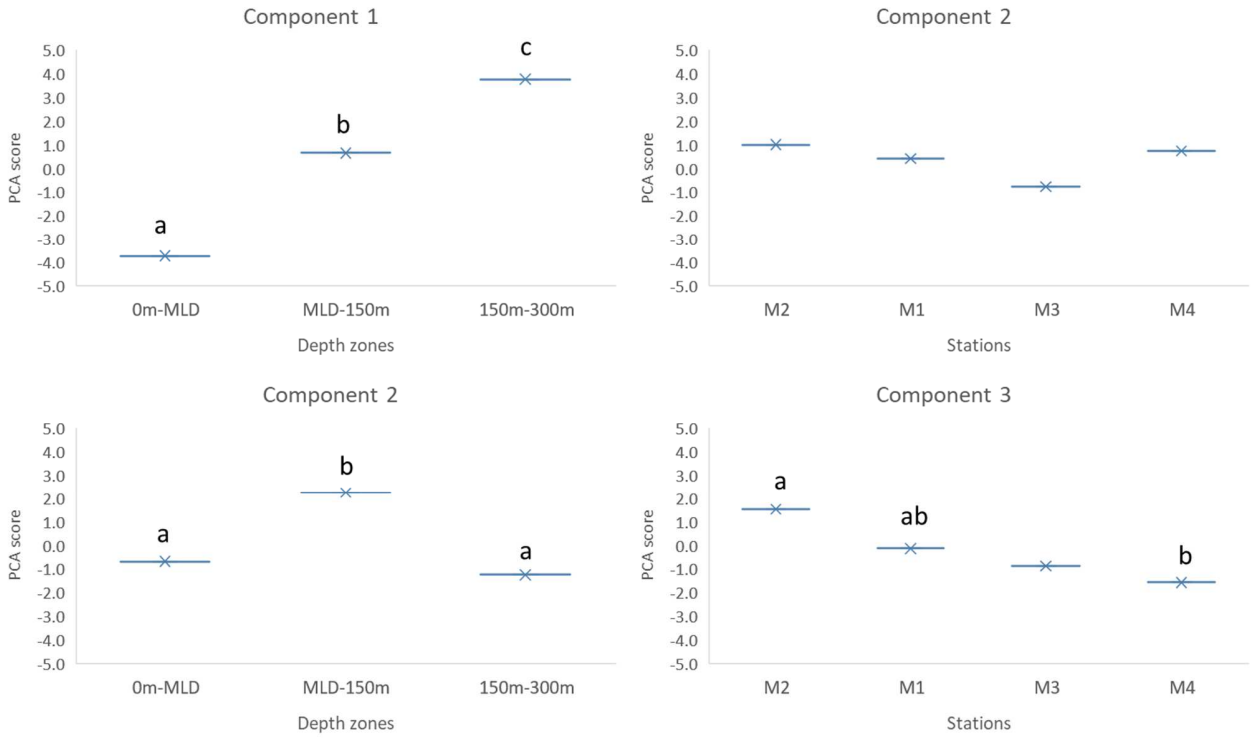

Figure 5: (Left) Non-parametric analysis of variance with PC1 and PC2 as the dependent variables (all stations pooled) and depth intervals as the independent variable; (Right) Non-parametric analysis of variance with PC2 and PC3 as the dependent variables (all depth intervals pooled) and stations as the independent variable. Letters a, b and c indicate statistical differences among conditions.

420

FA variability according to depth and stations

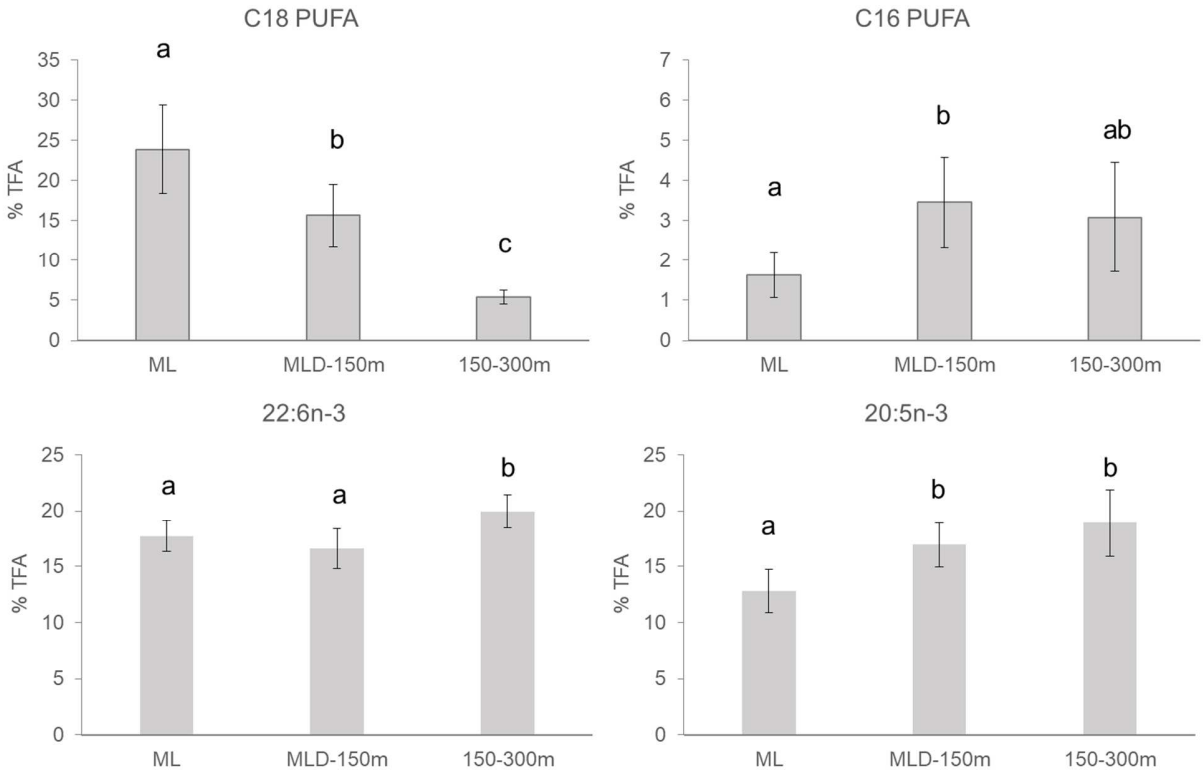

Figure 6: Percentages (relative to TFA) of C18 PUFA (sum of 18:3n-3, 18:4n-3 and 18:5n-3), C16 PUFA (sum of 16:2n-7, 16:2n-4, 16:3n-4 and 16:4n-1), 22:6n-3 and 20:5n-3 according to depth intervals. Letters a, b and c indicate statistical differences among conditions.

Furthermore, we explored the relationships between proportions of individual FA and depth (considering all stations together). Depth explained significantly the variability of 17:1n-7 (R^2=61%, p<0.0001), 18:2n-6 (R^2=30%, p<0.001), 18:3n-6 (R^2=37%, p<0.001), 18:3n-3 (R^2=44%, p<0.0001), 18:4n-3 (R^2=49%, p<0.0001), 18:5n-3 (R^2=44.7%, p<0.0001) through negative linear regressions. R^2 values were improved using Log regression for 18:2n-6 (R^2=50%, p<0.0001), 18:3n-3 (R^2=61%, p<0.0001), 18:4n-3 (R^2=68%, p<0.0001), 18:5n-3 (R^2=68%, p<0.0001). At the opposite, depth explained significantly the variability of 16:0 (R^2=68%, p<0.0001), 18:1n-9 (R^2=56%, p<0.001), 20:1n-9 (R^2=78%, p<0.0001), 22:1n-7 (R^2=41%, p<0.0001), 22:1n-9 (R^2=36%, p<0.001), and 22:5n-3 (R^2=79%, p<0.0001), through positive linear regressions. The best fitting regressions for 18:4n-3, 18:5n-3, 20:1n-9 and 22:5n-3 as a function of depth are presented in Figure S1. Variations according to depth concerned also LC-PUFA 20:5n-3 and 22:6n-3, and diatom C16 PUFA (the sum of 16:2n-

7, 16:2n-4, 16:3n-4 and 16:4n-1) as illustrated in Figure 6 for the three depth intervals considered. Averaged proportions of 20:5n-3 and diatom C16 PUFA were significantly higher in the MLD-150m and 150-300m depth intervals in comparison to the ML. For 22:6n-3, relative proportions remained high throughout the upper water column (0-300m) ranging from 18 to 20% of TFA, and were significantly higher in the deepest depth zone (150-300m).

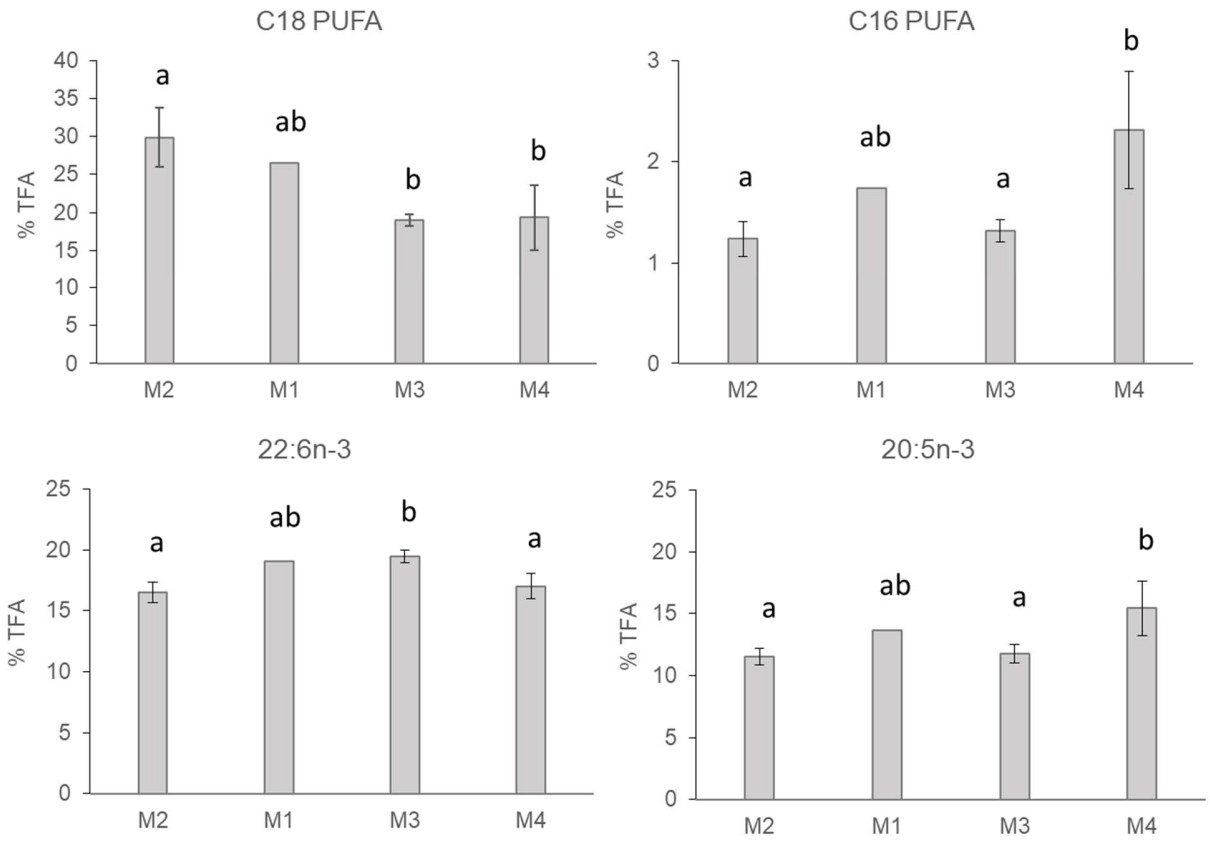

Figure 7: Percentages (relative to TFA) of C18 PUFA (sum of 18:3n-3, 18:4n-3 and 18:5n-3), C16 PUFA (sum of 16:2n-7, 16:2n-4, 16:3n-4 and 16:4n-1), 22:6n-3 and 20:5n-3 according to stations in the ML. Letters a and b indicate statistical differences among conditions.

Considering the significant differences between depth intervals, we compared FA profiles among stations within depth zones (Figure 7 for the ML). In the ML, the sum of 18:3n-3, 18:4n-3 and 18:5n-3 proportions was significantly higher at M1 and M2 stations compared to M3 and M4 stations off the plateau. The sum of diatoms C16 PUFA (16:2n-7, 16:2n-4, 16:3n-4 and 16:4n-1) and the

proportion of 20:5n-3 were significantly higher at station M4 than at stations M2 and M3. No difference among stations were found within both MLD-150m and 150m-300m zones.

To attempt explaining difference of FA composition among stations, relationships between physico-chemical parameters and FA composition were explored. We only considered regressions with $R^2 > 40\%$ with p value <0.01. Diatoms C16 PUFA and 20:5n-3 proportions were statistically negatively correlated to temperature (R^2=47% and 44%, respectively, with p <0.01, Figure S2). The sum of 18:3n-3, 18:4n-3 and 18:5n-3 was positively correlated to NH_4^+ (R^2=41%, p<0.01, Figure S2).

Diatom C16 PUFA and 20:5n-3

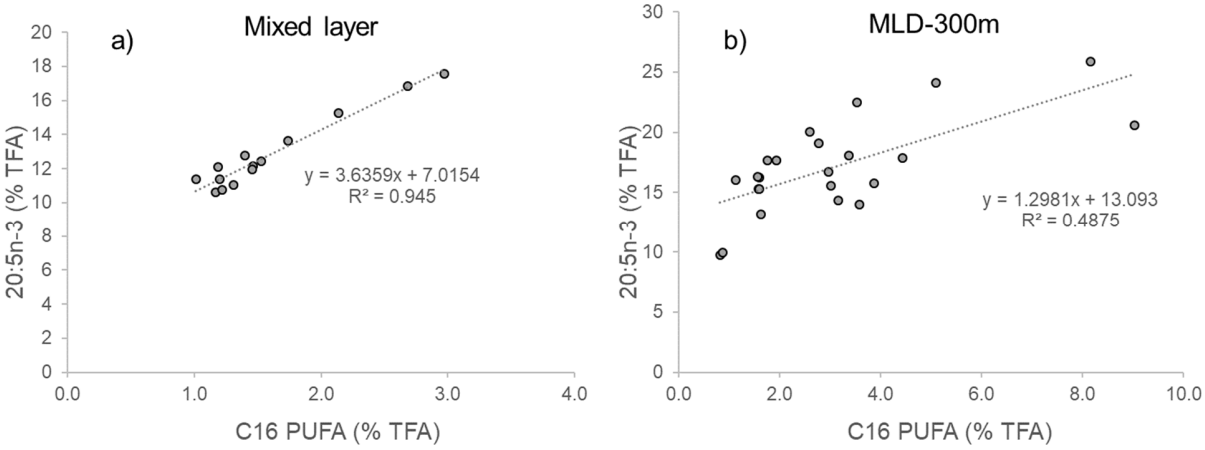

Figure 8: Correlation between diatoms C16 PUFA and 20:5n-3 proportions (% of total fatty acid-TFA) for the mixed layer (ML) (a) and for ML depth (MLD)-300m depth interval (b).

As diatoms C16 PUFA and 20:5n-3 were gathered in the PCA, we explored further this relationship in Figure 8. For the ML (Fig. 8a), C16 PUFA and 20:5n-3 appeared highly related regardless of stations (R^2=0.945, p<0.001). The slope of the regression indicated an average ratio of 20:5n-3 to C16 PUFA of 3.6±0.2, substantially higher than the ratio obtained for four diatom classes (Bacillariophyceae, Cosciondiscophycea, Fragilariophycea, and Mediophycea) gathered from literature (see Table S1), which ranged from 0.9 to 1.6. Considering the MLD-300m depth interval (Fig. 8b), the correlation between C16PUFA and 20:5n-3 was lower but still significant (R^2=0.487, p<0.001) and the average 20:5n-3 to C16 PUFA ratio decreased to 1.6±0.2.

458 **n-3 C18 PUFA and 22:6n-3**

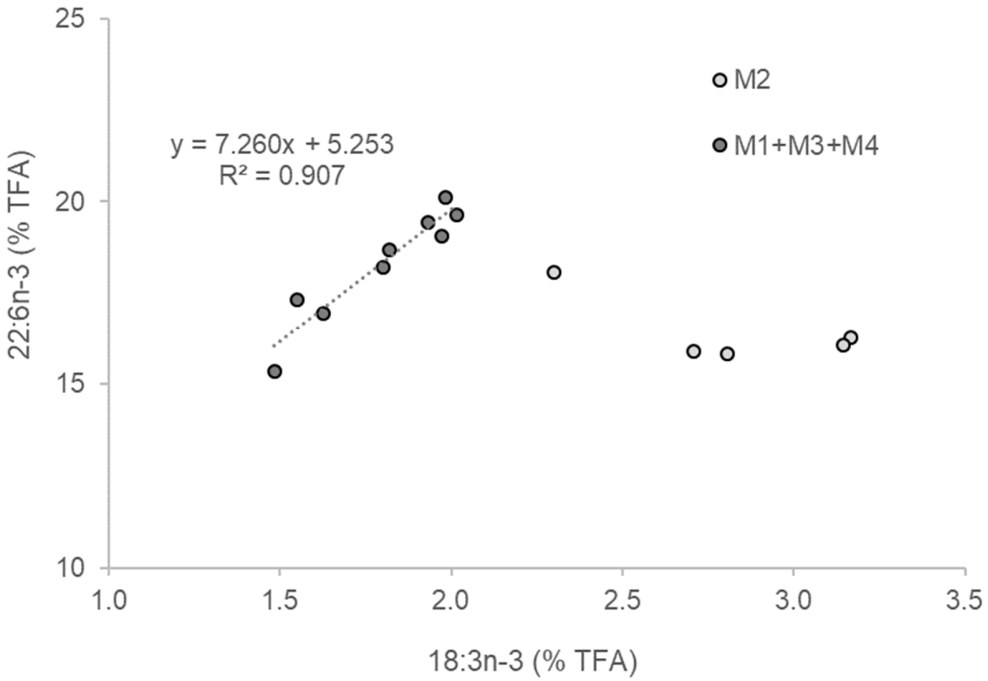

Figure 9: Linear regressions between 18:3n-3 and 22:6n-3 (% total fatty acid-TFA) in the mixed layer for off-plateau stations (M1, M3 and M4) and on-plateau station (M2).

459 From the PCA, 22:6n-3 was poorly correlated to axis 1 (R^2=12.5%, $p<0.05$) and not correlated
460 to axes 2 and 3 when considering all stations and depths together. To further explore the
461 relationship with non-diatom markers, we plotted in Figure 9 18:3n-3 against 22:6n-3 proportions
462 in the ML. Although the numbers of data points reduced its statistical strength, separating the
463 samples according to station locations (off-Plateau versus on-Plateau) allowed to obtain a
464 significant (R^2=0.907, $p<0.001$) positive relationship between 18:3n-3 and 22:6n-3 for off-plateau
465 stations (M1, M3, and M4). For the on-plateau station M2, the relationship was not significant
466 ($p=0.17$) although 18:3n-3 and 22:6n-3 were negatively correlated.

467 22:6n-3 to n-3 C18 PUFA ratio increased linearly with depth between the surface and 300 m
468 (R^2=0.726, $p<0.0001$; Figure 10). Significant relationships were observed between 22:6n-3/n-3 C18

469 PUFA ratio and 22:5n-3 and 20:1n-9 (R^2=0.874 with p<0.0001 and R^2=0.551 with p<0.001,
470 respectively) are shown in Figure S3.

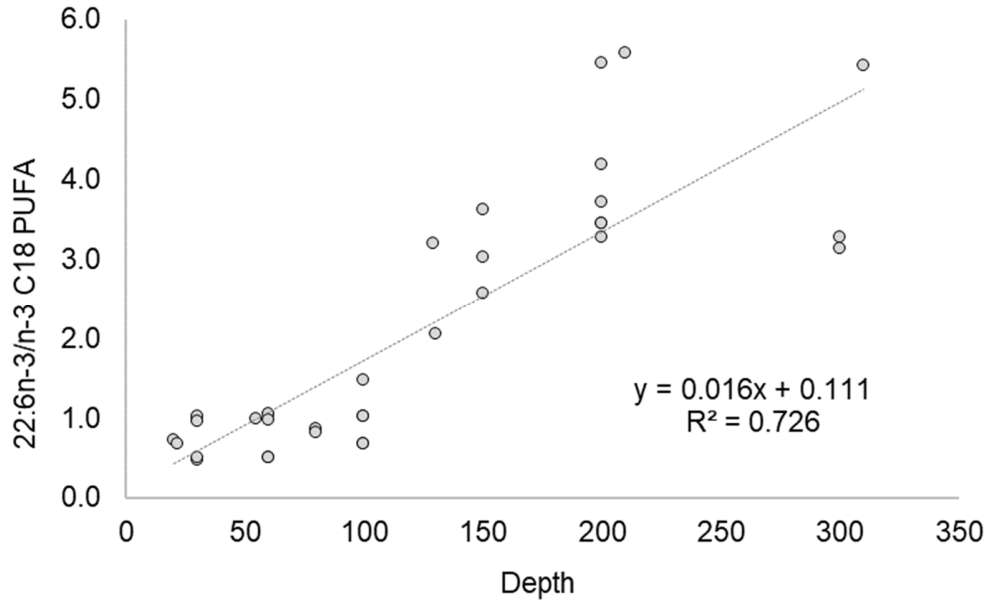

Figure 10: Linear regression between 22:6n-3 to n-3 C18 PUFA ratio according to depth (m).

471

FA-based nutritional quality of SPOM

The nutritional quality index (NQI) deduced from FA is presented in Figure 11. NQI ranged from 354 to 477 (average 394±37) and did not vary significantly according to depth zones. It has to be noted that NQI was more variable with increasing depth. When considering together the three depth zones, NQI was slightly higher on-plateau than off-plateau.

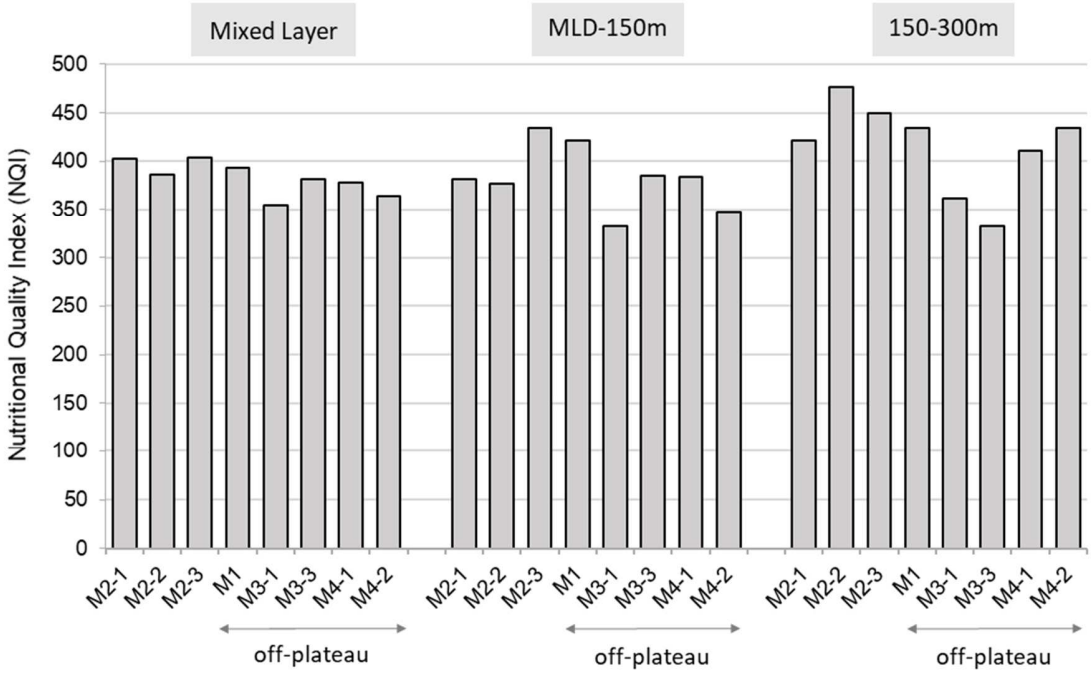

Figure 11: FA-based nutritional quality index of SPOM (1-50 μm) according to stations and depth intervals.

D. Discussion

This study investigated the upper water column distribution of 36 FA in SPOM (1-50 μm) collected in the Indian sector of the Southern Ocean in the region of Kerguelen Islands. Principal component analysis (PCA) revealed contrasted FA profiles attributable to depth for both PC1 and 2. The PC3 also revealed significant differences between HNLC stations M3 and M4 and the naturally-iron fertilized station M2. In the following, we discuss first how the post-bloom phytoplanktonic community and depth impact the FA composition of SPOM in terms of SC-PUFA and MUFA. We then consider the potential sources of essential LC-PUFA, 20:5n-3 and 22:6n-3, in

485 the ML and their fate in the upper mesopelagic. Finally, the FA-based nutritional quality of SPOM
486 is discussed according to depth and stations location.

487 **Post-bloom phytoplankton community and FA profiles**

488 The MOBYDICK survey took place in late summer/early autumn coinciding with post-bloom
489 conditions on and off the Kerguelen Plateau. Chl-a was low in the ML (<0.6 $\mu g.L^{-1}$), and POC and
490 TFA concentrations were <45 $mg.L^{-1}$ and <4.5 $\mu g.L^{-1}$, respectively. The phytoplanktonic
491 community, as described using 18S rDNA amplicon sequencing, pigments, flow cytometry, and
492 microscopic enumeration (Irion et al., 2021, 2020; Lafond et al., 2020), revealed a mixed
493 composition with three main groups, prymnesiophytes, diatoms and prasinophytes showing
494 variable proportions on- and off the Plateau. Nano-phytoplankton (prymnesiophytes) were the
495 most abundant group (37–53% and 59–70% of total Chl-a on- and off-plateau, respectively)
496 followed by diatoms (27-40% and 18-33% of total Chl-a on- and off-plateau, respectively), and
497 finally by pico-phytoplankton (prasinophytes) (Irion et al., 2021, 2020). This latter group was
498 found in low proportions at all stations except on the plateau where it reached up to 16% of total
499 Chl-a at the end of the survey (M2-3) (Irion et al., 2020). The mixed composition of the
500 phytoplankton community was well reflected in the FA profile of SPOM, especially when
501 considering chloroplastic C16 and n-3 C18 PUFA (Alonso et al., 1998; Guschina and Harwood,
502 2006), which derive mainly from autotrophic biomass. n-3 C18 PUFA (sum of 18:3n-3, 18:4n-3, and
503 18:5n-3) are characteristic of non-diatom phytoplankton including prymnesiophytes (24% of n-3
504 C18 PUFA) and prasinophytes (42% n-3 C18 PUFA), and were particularly abundant in the ML
505 representing between 17 to 32% of TFA. n-3 C18 PUFA in the ML were significantly ($p<0.05$)
506 higher on the Plateau (30±4% on average at station M2) and downstream (26% at M1) in
507 comparison to HNLC off-plateau stations (19±4% on average at stations M3 and M4). On the
508 Plateau, n-3 C18 PUFA increased from 22% (M2-1) to 32% (M2-2 and M2-3) during the survey
509 probably illustrating the increasing proportion of Prasinophytes.

510 For diatoms, their abundance could be identified using C16 PUFA (sum of 16:2n-7, 16:2n-4,
511 16:3n-4 and 16:4n-1), which are highly specific to this phylum with an averaged proportion of
512 16±4% (see Table S1 for details). Diatom C16 PUFA were found at all stations in the ML. C16 PUFA

were the lowest on the Plateau at station M2 (1.2±0.2% on average) and upstream at station M3 (1.3±0.2% on average) and were significantly ($p<0.05$) higher upstream at station M4 (2.3±0.6% on average) compared to the other stations. Variability of C16 PUFA according to stations in the ML could be compared to estimates of diatom abundance deduced from pigments (Irion et al., 2020), diatom biomass contribution to POC as well as BSi (Lafond et al., 2020). For off-plateau stations (M1, M3, and M4), C16 PUFA matched the trends in BSi concentrations (2.2 $\mu mol.L^{-1}$ at M4 > 1.0 $\mu mol.L^{-1}$ at M1 > 0.4 $\mu mol.L^{-1}$ at M3) as well as diatom contribution to POC (24±6% at M4 > 16±1% at M1 > 6±2% at M3). On the Plateau, differences arose and C16 PUFA proportions were the lowest while diatoms were found to be more abundant, 27-40% of total Chl-a (Irion et al., 2020) and 17 to 43% of POC (Lafond et al., 2020). This was especially the case at the last visit on the Plateau (station M2-3), where a bloom of *Corethron inerme* was observed (Lafond et al., 2020) which contributed to an increase of TFA and POC concentrations (2.1 to 2.9 $\mu g.L^{-1}$ and 27 to 40 $\mu g.L^{-1}$, respectively). In contrast, this effect was not reflected in C16 PUFA, whose proportions stayed relatively stable between station M2-2 (1.0%) and M2-3 (1.2%). This pattern could indicate that this late summer diatom bloom was probably poor in chloroplastic C16 PUFA.

Changes in FA profiles with depth

Below the ML, TFA and POC decreased rapidly and substantial changes were evidenced at all stations with a consistent decrease in n-3 C18 PUFA (from 24 ± 6% in the ML to 16 ± 6% in the MLD-150m down to 5 ± 1% in the 150-300 m depth zones) and an increase in C16 PUFA (from 1.6 ± 0.6% in the ML to 3.5 ± 1.1% in the MLD-150m and to 3.1 ± 1.4 % in the 150-300 m intervals). The observed pattern in phytoplankton-derived FA was in agreement with the vertical distribution of pigments showing a rapid decrease in prymnesiophytes pigments below the ML and an increasing contribution of diatom pigments, the latter representing up to 77-96% of total Chl-a at 250 m depth (Irion et al., 2021). In addition, we noted variable vertical trends of n-3 C18 PUFA and C16 PUFA as observed with pigments (Irion et al., 2021). On the Plateau and downstream (Station M2 and M1) n-3 C18 PUFA decreased rapidly below the MLD, while at station M3 C18 PUFA remained relatively high in the MLD-150m depth interval (22% on average) and decreased only below 150 m (6% on average). For C16 PUFA and diatoms, the increase with depth was

particularly rapid on the Plateau at the first two visits (1.5 to 5.5% at M2-1 and 1.0 to 4.3% at M2-2 between the ML and the MLD-150m depth zone) indicating an important accumulation of diatoms just below the MLD. Considering that biomass and associated FA increased below the ML as a result of vertical transfer from the surface, the observed trends in n-3 C18 PUFA and C16 PUFA proportions may be consistent with a more efficient export of diatoms in comparison to nano- and pico-phytoplankton below the ML. This feature is commonly observed in the SO (Salter et al., 2012, 2007) and was documented in details on the Plateau (Blain et al., 2021; Rembauville et al., 2015a, 2015b) and also in the surrounding HNLC areas (Rembauville et al., 2017).

Unexpectedly and along with n-3 C18 PUFA, the MUFA 17:1n-7 decreased linearly with depth. As its distribution was concomitant with the one of chloroplastic n-3 C18 PUFA, it suggested its production was mostly autotrophic and occurred in the ML. 17:1n-7 is not listed in the meta-analysis of Jónasdóttir (2019) and Cañavate (2019) and is only rarely cited in papers analyzing FA in phytoplankton species. The cyanobacteria *Synechococcus elongates*, *Microcystis aeruginosa* and *Anabaena variabilis* were reported to contain respectively 0.6%, 0.5% and 1.3 of 17:1n-7 (Bec et al., 2006; Martin-Creuzburg et al., 2008). Interestingly, the heterotrophic nanoflagellates *Paraphysomonas sp.*, concentrated this MUFA at 3.4% and 1.5%, when fed *S. elongates*, *M. aeruginosa*, respectively (Bec et al., 2006). Indeed, these planktonic groups were observed during the MOBYDICK survey. Heterotrophic nanoflagellates, pico and nano-plankton varied between 3.3 and 4.7 10^6 cells.L^{-1}, 0.8 and 2.0 10^6 cells.L^{-1}, and 73 and 111 10^3 cells.L^{-1} respectively, in the ML (Christaki et al., 2020). However, while heterotrophic nanoflagellates were more abundant at M2 than at off-plateau stations (M3 and M4) (Christaki et al., 2020), no significant difference was observed according to stations for both concentration (in $\mu g.L^{-1}$) and relative proportion of 17:1n-7.

The long chain MUFA 20:1n-9, 22:1n-7 and 22:1n-9, which are mainly produced by zooplankton such as calanoid copepods and other crustaceans (Brett et al., 2009; Dalsgaard et al., 2003; Kattner and Hagen, 1995; Mayzaud et al., 2007; Parrish, 2013; Wilson et al., 2010) can be used to detect potential interactions with zooplankton via the production of fecal pellets and their presence into SPOM (Mayzaud et al., 2007; Sheridan et al., 2002; Wilson et al., 2010). Fecal pellets

569 are known to play an important role in the vertical transfer of OM in the Kerguelen region
570 (Ebersbach and Trull, 2008; Laurenceau-Cornec et al., 2015), particularly on the Plateau during the
571 post-bloom period (Rembauville et al., 2015a). In our samples, long chain MUFA 20:1n-9, 22:1n-7
572 and 22:1n-9 were detected at all stations, their proportions were low in the ML (sum of 20:1n-9,
573 22:1n-7, and 22:1n-9 ranging between 0.11 and 0.25%) and increased linearly with depth (R^2=0.683,
574 $p<0.0001$) reaching the highest values in the 150-300m depth zone (range: 0.21-0.61%). Although
575 particularly low, these proportions still appeared comparable to those measured in fecal pellets
576 of copepods and euphausiids (range: 1.3-2.2%) sampled in the Subantarctic zone of the SO
577 (Mayzaud et al., 2007). This could indicate that a fraction of the SPOM sampled during the post-
578 bloom period was composed of fecal material excreted by zooplankton, which increased with
579 depth. Moreover, and as outlined in the PCA, the PUFA 22:5n-3 was clearly associated with long
580 chain MUFA. Indeed, a similar linear increase of 22:5n-3 with depth (R^2=0.79, $p<0.001$) was
581 reported suggesting a common origin. This PUFA can be formed from the 20:5n-3 through
582 elongation and could be a synthesis intermediate of 22:6n-3 in crustaceans including copepods
583 (Kabeya et al., 2021; Monroig and Kabeya, 2018; Nielsen et al., 2019). This PUFA was found in
584 three zooplankton species *Themisto libellula*, *Calanus marshallae/glacialis* (*Calanus spp.*), and
585 *Thysanoessa raschii* collected in the Bering Sea and ranged between 0.5-0.6% of TFA (Wang et al.,
586 2015). As part of MOBYDICK, 22:5n-3 accounted on average for 0.77% of total phospholipids
587 extracted from 70 zooplankton samples (Puccinelli E. in prep) and its abundance in SPOM reached
588 1.3±0.1% on average in the 150-300m depth interval.

589 **Origin and fate of 20:5n-3**

590 Synthesis of the LC-PUFA 20:5n-3 is assumed to occur essentially via autotrophy and can be
591 performed by several phytoplankton phyla such as Diatoms, ochrophytes, haptophytes, and
592 rhodophytes (see Table S1 for details). In the ocean and in particular the SO, the main suppliers
593 of 20:5n-3 are generally considered to be diatoms (Ericson et al., 2018; Hellessey et al., 2020). In
594 the case of MOBYDICK and for the Kerguelen area, this assumption seems to be true. 20:5n-3 was
595 clearly associated with diatom C16 PUFA in the PCA and furthermore in the ML, proportions of
596 20:5n-3 appeared tightly related to C16 PUFA through a positive linear correlation (R^2=0.945,

597 $p<0.05$) regardless of stations. Abundance of 20:5n-3 accounted for a significant contribution to
598 TFA in the ML (13±2% on average), highest proportions were found at station M4 (15±2% on
599 average), significantly ($p<0.001$) different in comparison to stations M2 and M3 (12±1% on average
600 at both stations) and to a lesser extent to station M1 (14% on average). Measured proportions in
601 1-50 µm SPOM were comparable to literature data for diatoms ranging from 15 to 20% of 20:5n-3
602 (see details in Table S1). However, the literature range corresponds to diatoms monoculture and
603 differs from the MOBYDICK situation. Because diatoms were a minor group in the ML (18–40%
604 of total Chl-a) (Irion et al., 2020), proportions of 20:5n-3 in SPOM are expected to be lower
605 compared to literature data if only provided by diatoms. Based on the highly significant linear
606 relationship ($p<0.001$) between 20:5n-3 and diatoms C16 PUFA in the ML, we calculated a 20:5n-
607 3/C16 PUFA ratio of 3.6±0.2, which appeared to be ~2 fold higher compared to literature data
608 (average of 1.5 calculated from Table S1). This difference suggests that the diatom community of
609 the Kerguelen region, both on and off-Plateau, had higher proportions of 20:5n-3 than cultured
610 diatoms. Such a case was previously reported by Vaezi et al. (2013), who found that the cold-water
611 *Fragilariopsis cylindrus* was able to produce up to 31.4% of 20:5n-3, approximately twice the
612 average value usually found in the literature (Table S1). Additionally, we reported a significant
613 negative regression between 20:5n-3 and temperature in the ML ($R^2=44\%$, $p<0.01$). Indeed, 20:5n-
614 3 proportion was the highest at station M4 where temperature was the lowest. Based on literature
615 data, Hixson and Arts (2016) established a negative linear regression between temperature and
616 20:5n-3 in diatoms. Thus, it can be speculated that the high 20:5n-3 content in diatoms of the
617 Kerguelen region partially reflected homeoviscous adaptation to low temperatures.

618 In the upper mesopelagic, relative proportions of 20:5n-3 increased, reaching 17±2% in the
619 MLD-150m zone and 19±3% in the 150-300m zone, and were significantly ($p<0.001$) different
620 compared to the ML. Linear relationship between C16 PUFA and 20:5n-3 was still significant
621 below the MLD ($R^2=0.487$, $p<0.001$) with an average ratio 20:5n-3/C16 PUFA of 1.3. This ratio was
622 lower than in the ML and closer to the literature value (1.5, calculated from Table S1). This
623 suggests that the vertical distribution of 20:5n-3 was still mostly determined by the fate of diatoms
624 in the mesopelagic with no significant difference among stations. Accordingly, trends in 20:5n-3
625 proportions were likely a result of the increasing proportion of diatoms observed below the MLD.

However, according to the low 20:5n-3/C16 PUFA ratio, the FA composition of diatoms has probably been modified with depth, and this could be related to several factors. For instance, diatoms assemblages exhibited consistent variations according to stations and depth (Lafond et al., 2020). This was particularly the case at the plateau station M2, where in the ML diatom biomass was dominated by the large centric *Corethron inerme* (59 to 83% of diatom biomass), while below the ML, *Eucampia antarctica* at the first visit (M2-1), and *Chaetoceros* resting spores and *Chaetoceros spp.* at the following visits (M2-2 and M2-3) were the dominant contributors (Lafond et al., 2020). At other stations, the community structure was more diverse and included *Actinocyclus spp.*, *Thalassiosira spp.*, *Chaetoceros atlanticus* and *Chaetoceros* resting spores (Lafond et al., 2020). Considering that the amount of 20:5n-3 produced varies at a species level, diatom diversity were thus likely to influence the FA content available. Other factors could also involve the physiological state of diatom cells, which greatly evolved in the upper mesopelagic zone as a consequence of grazing, parasitic infection and mortality (Lafond et al., 2020; Sassenhagen et al., 2020). Indeed, abundance of detrital cells in the form of empty, broken or crushed frustules rapidly increased below the ML and this was particularly pronounced at off-plateau stations M1, M3, and M4 in comparison to on-plateau station M2, where up to 48% of cells were still intact between 175-200 m depth (Lafond et al., 2020). Finally, the relative proportions of 20:5n-3 as well as 20:5n-3/C16 PUFA ratio could have been modified as a result of the increasing proportion of fecal material observed in the mesopelagic zone. The FA composition of fecal pellets reflects the composition of the zooplankton organism (Hamm et al., 2001; Mayzaud et al., 2007) and can contain high and variable proportions of 20:5n-3 (up to 25-30%) as observed in krill (Hellessey et al., 2020), with substantial differences in comparison to the phytoplankton food source.

Origin and fate of 22:6n-3

The LC-PUFA 22:6n-3 is also produced at the basis of the marine food web by unicellular eukaryotic organisms (Dalsgaard et al., 2003; Parrish, 2013) and it is produced by several phytoplankton taxa (as detailed in Table S1). The taxa with the highest 22:6n-3 proportions, grown in autotrophic conditions, include Dinophyceae (17.5% in average), Coccolithophyceae (11.6% in average) and Prymnesiophyceae (10.7% in average) and exclude diatoms, which produce only

small amounts of 22:6n-3 (<2.5%). In this study and considering first the ML, where autotrophic production was likely dominant, the 1-50 µm SPOM was found to be rich in 22:6n-3 at all stations representing 18±1% on average. The highest proportions were found off the Plateau at stations M1 and M3, with 19.1% and 19.5±0.5%, respectively, which were slightly higher to the upstream station M4 (17.0±1.0% in average) and the on-plateau station M2 (16.4±0.8% in average). According to the composition of the post-bloom phytoplankton community (Irion et al., 2021, 2020), it can be hypothesized that Prymnesiophycea, as the dominant group, were the most important suppliers of 22:6n-3 in the ML both on and off-Plateau. Autotrophic dinoflagellates (Dinophyceae), which are generally considered as important producers in the SO (Dalsgaard et al., 2003; Ericson et al., 2018; Falk-Petersen et al., 2000) were likely marginally involved as their contribution to the phytoplankton community was very modest (Irion et al., 2020). In addition to Prymnesiophyceae, contribution of pico-phytoplankton (Prasinophyceae) to 22:6n-3 proportions was also probable, especially on the Plateau where they were more abundant. Prasinophyceae are able to produce 22:6n-3 but in much lower proportions (7.0%) compared to Prymnesiophyceae. In order to test the assumption that Prasinophyceae and Prymnesiophyceae contributed to 22:6n-3 production, we considered the relationship between 22:6n-3 and 18:3n-3 in the ML. 22:6n-3 appeared strongly related to 18:3n-3 only at off plateau stations (M1, M3, and M4) through a positive correlation (R^2=0.907, $p<0.05$). The slope of the regression corresponding to the averaged 22:6n-3/18:3n-3 ratio found in off Plateau SPOM was 7.2 and was substantially higher than the ratio deduced from literature data for Prymnesiophycea (2.1) and Prasinophycea (0.6). The fact that the SPOM 22:6n-3/18:3n-3 ratio was closer to that of Prymnesiophyceae may indicate that 22:6n-3 was at least partially produced by Prymnesiophyceae rather than Prasinophyceae at these off-Plateau stations. The situation was markedly different on the Plateau at station M2, where 22:6n-3 and 18:3n-3 were negatively related but not significantly, suggesting a more complex pattern. The observed trend in SPOM could be consistent with a multiple origin of 22:6n-3 with some from Prymnesiophyceae having a high 22:6n-3/18:3n-3 ratio and some from Prasinophyceae having a low 22:6n-3/18:3n-3 ratio. Different contributions of Prymnesiophycea and Prasinophyceae on and off Plateau seemed to be confirmed by the decrease of 22:6n-3/18:3n-3 ratio in SPOM observed at station M2 according to visits (7.9 at M2-1, 5.7 at M2-2, and 5.1 at M2-3)

683 which fits with the increasing proportion of Prasinophyceae deduced from pigments and reaching
684 up to 16% of total Chl-a at M2-3 (Irion et al., 2020).

685 Considering Prymnesiophycea, it is worth noting that this group was mostly composed by a
686 single species, *Phaeocystis antarctica* (Irion et al., 2020), whose FA profile remains to be
687 documented. As a comparison, data available for other species of *Phaeocystis* (*pouchetti* and *globosa*)
688 exhibit contrasted FA profiles, with some studies reporting only trace or minor amounts of 22:6n-
689 3 (maximum 6.2% TFA) (Claustre et al., 1990; Nichols et al., 1991; Skerratt et al., 1995), while others
690 reported much higher proportions, up to 15% (Hamm et al., 2001; Sargent et al., 1985; Virtue et
691 al., 1993). In our case, *Phaeocystis antarctica* was necessarily high in 22:6n-3 to match the high
692 proportions observed in the ML (18±1% on average) and further work is needed to confirm this
693 hypothesis.

694 In addition to autotrophic origin, trophic upgrading by heterotrophic protists such as
695 dinoflagellates and ciliates, which composed the microzooplankton, may also have contributed to
696 the observed 22:6n-3 content in the ML (Broglio et al., 2003; Lund et al., 2008). Heterotrophic
697 dinoflagellates and ciliates were documented at both on and off-plateau stations and ranged
698 between 0.29 and 2.3 10^3 cells L^{-1} (Christaki et al., 2021). Dinoflagellates, dominated by
699 *Gymnodinium* sp., were more abundant than ciliates at all stations and grazed actively on
700 phytoplankton with grazing rates exceeding phytoplankton growth rates (Christaki et al., 2021).
701 Heterotrophic dinoflagellates can contain especially high proportions of 22:6n-3, >40% as reported
702 by Lim et al. (2020) for *Gymnodinium smaydae*, and up to >50% for *Crypthecodinium cohnii* (Jiang
703 and Chen, 2000). Interestingly for this latter species, 22:6n-3 proportions were dependent on
704 cultivation temperature, increasing from 17% to 53% with decreasing temperature from 30°C to
705 15°C (Jiang and Chen, 2000). Considering the low temperature environment of the Kerguelen
706 region, this may have favored high 22:6n-3 proportions in heterotrophic protists. Another
707 characteristic of heterotrophic dinoflagellates is their low content in chloroplastic n-3 C18 PUFA
708 and as a consequence, their high 22:6n-3/n-3 C18 PUFA ratio (Lim et al., 2020; Lund et al., 2008).
709 As an example, *Gymnodinium smaydae* had a 22:6n-3/18:3n-3 ratio >80, much higher than the ratio
710 of its prey *Heterocapsa rotundata* of 5.4 (Lim et al., 2020). This may be one explanation for the higher

711 22:6n-3/18:3n-3 ratio found in the ML (7.2) in comparison to autotrophic producers (0.6-2.1) and
712 could be consistent with a small contribution (<10%) of heterotrophic protists to 22:6n-3 content.

713 Below the ML in the upper mesopelagic, 22:6n-3 concentrations (in $\mu g.L^{-1}$) decreased
714 substantially and similarly to TFA concentrations (R^2=0.975, $p<0.05$) it was maintained at high
715 relative proportions with 17±2% in the MLD-150m depth interval comparable to the ML, and up
716 to 20±2% in the 150-300m depth interval, significantly ($p<0.001$) higher in comparison to the upper
717 layers. This vertical trend was in a marked contrast compared to n-3 C18 PUFA, which decreased
718 substantially both in concentration and proportion below the ML. This contrasted pattern was
719 initially outlined by the PCA, where 22:6n-3 was not correlated to any of the three axes and
720 furthermore, not associated to n-3 C18 PUFA when considering the whole dataset. These different
721 trends clearly indicate that the fate of 22:6n-3 in the mesopelagic could not be governed by the
722 vertical transfer of non-diatom phytoplankton which was initially involved in its production in
723 the ML, and most probably relied on another pathway. This pathway is further supported by the
724 linear increase of 22:6n-3 to n-3 C18 PUFA ratio according to depth (R^2=0.726, $p<0.0001$) indicating
725 a progressive enrichment of 22:6n-3 compared to n-3 C18 PUFA in SPOM between the surface and
726 300 m depth. Moreover, this increase correlates fairly well with the heterotrophic FA 22:5n-3
727 (R^2=0.874, $p<0.0001$) and also but to a lesser extent with the MUFA 20:1n-9 (R^2=0.551, $p<0.001$).
728 Variations of 22:5n-3 and 20:1n-9 were attributed earlier in the discussion to an increasing
729 abundance of fecal material at depth. Accordingly, it can be postulated that 22:6n-3 in SPOM may
730 be at least partially associated with this fecal material in the upper mesopelagic and thus its fate
731 may be controlled by interactions with the heterotrophic food web. It is worth noting that
732 correlations were made regardless of stations, indicating that this potential transfer pathway
733 seemed to affect both iron-fertilized and HNLC regions. Such an association of 22:6n-3 with fecal
734 material has already been documented in some regions of the world ocean, including the high
735 latitude North Pacific where fecal OM and high proportions of 22:6n-3 (range 8-17% of TFA) were
736 evidenced throughout the water column (Sheridan et al., 2002; Wilson et al., 2010) and also in the
737 Arctic, where it was demonstrated that 22:6n-3 rich OM (~20% of TFA) derived from *Phaeocystis*
738 *pouchetii,* was exported below the euphotic zone via krill fecal strings (Hamm et al., 2001).

739 In the present case, the processing of 22:6n-3 from phytoplankton to suspended fecal material
740 is likely to be complex and could involve a number of heterotrophic intermediates. Among
741 grazers, mesozooplankton such as copepods and other large size crustacean zooplankton require
742 to be considered as C20-C22 MUFA are representative of fecal material excreted by these
743 organisms (Brett et al., 2009; Dalsgaard et al., 2003; Kattner and Hagen, 1995; Mayzaud et al., 2007;
744 Parrish, 2013; Wilson et al., 2010). Mesozooplankton were documented at all stations and
745 exhibited significant variations according to sites and visits from 207 ind.m^{-3} at M2–1 to 1636
746 ind.m^{-3} at M4–1 (Christaki et al., 2021). Moreover, grazing experiments showed that copepods
747 were not grazing directly on phytoplankton but were feeding primarily on microzooplankton
748 controlling their abundance during the post-bloom period (Christaki et al., 2021). This feeding
749 strategy on heterotrophic protists as well as the selective storage of 22:6n-3 as an essential LC-
750 PUFA for mesozooplankton (Arendt et al., 2005) may have favoured its accumulation relative to
751 n-3 C18 PUFA and as a result, impacted the composition of fecal material produced by these
752 organisms. In addition to mesozooplankton, other grazers such as salps may also be involved in
753 the channelling of 22:6n-3. Salps are important grazers of small phytoplankton (Moline et al., 2004)
754 and flagellates (Pakhomov and Hunt, 2017; von Harbou et al., 2011), and produce easily
755 fragmented tabular fecal pellets (Iversen et al., 2017). Salps population (*Salpa thompsoni*) were
756 particularly abundant on the Plateau at station M2 and downstream at station M1 representing
757 up to 40% of total micronekton biomass (Henschke et al., 2021).

758 **Nutritional food value according to production regimes**

759 The nutritional quality of OM as food for higher trophic levels is partly determined by the
760 abundance of the essential omega-3 LC-PUFA 20:5n-3 and 22:6n-3 and the essential omega-6
761 20:4n-6. In the present study, LC-PUFA essentially composed of omega-3 LC-PUFA were found
762 in high proportions, making up 27-44% of TFA, indicating a high nutritional value of SPOM both
763 in the ML and upper mesopelagic. Following the approach developed by Cañavate et al. (2019),
764 the NQI of SPOM was also high and ranged from 354 to 403 in the ML and from 333 to 477 in the
765 MLD-300m depth interval. As a comparison, much lower NQI were obtained in the estuary of
766 Guadalquivir River, with values always <200 (Cañavate et al., 2021), in the northern part of the

767 Indian sector of the ACC, with NQI of 193 and 242 in surface SPOM of the subtropical and
768 Subantarctic zone, respectively (Mayzaud et al., 2007), in the Northern Pacific, NQI was <300 in
769 >51 μm SPOM of the Subarctic area (Wilson et al., 2010) as well as in the coastal Antarctic zone,
770 NQI was <260 for a diatom sea-ice community of McMurdo Sound (Nichols et al., 1993). This
771 comparison confirms that quality of SPOM in the Kerguelen area was especially high in the post-
772 bloom period. High NQI values were observed over the whole area and seemed unrelated to the
773 contrasted productivity regimes that took place earlier in the season during the bloom. In the ML,
774 the high nutritional value of SPOM was mainly attributable to the mixed phytoplanktonic
775 community relying both on diatoms producing 20:5n-3 and small phytoplankton producing
776 22:6n-3. This mixed production of both LC-PUFA substantially promoted the nutritional quality
777 of SPOM and offered a valuable source of food for secondary consumers that could be of
778 importance for the ecosystem functioning.

779 In the upper mesopelagic, LC-PUFA in SPOM were maintained at similar, and even higher,
780 proportions in comparison to the ML (34±2% and 40±3% on average in the MLD-150m and 150-
781 300m depth intervals, respectively). Similarly, NQI remained high until 300 m depth (333-477)
782 even though TFA concentrations in seawater (in $\mu g.L^{-1}$) decreased substantially with depth. This
783 preservation of food quality in the upper mesopelagic was rather unexpected because LC-PUFA
784 are generally considered as a labile fraction of OM that could be easily degraded/consumed by
785 heterotrophic organisms during their transfer from the surface (Budge et al., 2006; Conte et al.,
786 2003, 1995; Wakeham, 1995). This is illustrated by the low NQI values that can be deduced from
787 sediment trap data, with values between 90 to 180 in trap samples collected between 50-100 m
788 depth in the North Atlantic (Budge and Parrish, 1998) and NQI <30 in samples collected at 300 m
789 depth in Breid Bay, Antarctica (Hayakawa et al., 1996). For the Kerguelen region, sediment trap
790 data obtained on the Plateau at station M2 (Rembauville et al., 2018) do not allow for NQI
791 estimates, however considering LC-PUFA concentrations per unit mass of OC, ranging from 0.03
792 to 3.4 $\mu g.mgOC^{-1}$ in the trap samples and from 14 to 44 $\mu g.mgOC^{-1}$ in our SPOM samples, it
793 appears that sinking material from traps was of much lower quality than suspended particles
794 collected on and off the Plateau. In the present case, the high quality of SPOM in the upper
795 mesopelagic could represent a valuable nutritional option for heterotrophic organisms residing

796 in the part of the water column and feeding on suspended particles such as zooplankton,
797 coprophages, detritivores, and bacteria.

798 ## E. CONCLUSION

799 In this study, FA distribution including essential LC-PUFA 20:5n-3 and 22:6n-3 was
800 documented in the upper water column of the Kerguelen Islands Region several weeks after the
801 bloom period in late summer/early autumn. Our results illustrate the important role of the mixed
802 phytoplankton community, composed of nano- and pico-size phytoplankton and diatoms, in
803 providing high proportions of both LC-PUFA to surface waters. Diatoms were identified as the
804 likely suppliers of 20:5n-3 and small phytoplankton (prymnesiophytes and prasinophytes)
805 supplying 22:6n-3. Elevated proportions are unrelated to past productivity regimes and were
806 observed both inside the iron-fertilized area on the Kerguelen Plateau (station M2) and
807 downstream (station M1), as well as outside in HNLC waters located upstream of the Plateau
808 (stations M3 and M4). As a consequence, and despite reduced productivity and biomass
809 abundance during the post-bloom period, phytoplankton-derived OM reveal an especially high
810 nutritional value that could be relevant for secondary consumers such as micro- and
811 mesozooplankton.

812 In the upper mesopelagic, both LC-PUFA were maintained at high relative proportions in
813 SPOM suggesting an efficient and probably fast vertical transfer from the surface. This vertical
814 transfer seems to proceed via distinct pathways according to LC-PUFA. For 20:5n-3, its fate in the
815 mesopelagic seems to mainly follow the one of diatoms and could be associated with the export
816 of large intact cells, diatoms aggregates as well as resting spores. For 22:6n-3, its fate with depth
817 appears not to be simply related to small phytoplankton but is most likely due to a complex
818 channeling through the heterotrophic food web resulting in its association with fecal material at
819 depth. Processing of 22:6n-3 could involve different intermediates such as heterotrophic protists
820 with dinoflagellates and ciliates (microzooplankton), which probably grazed on small
821 phytoplankton as well as larger zooplankton organisms such as copepods and salps, which
822 presumably fed on microzooplankton and produced fecal pellets rich in 22:6n-3. The complex
823 pathway of 22:6n-3 cannot be easily resolved using only SPOM data and additional evidences are

needed to better understand this pattern. Despite these contrasted pathways, FA-based nutritional quality of SPOM remained especially high in the upper mesopelagic and could represent an interesting food source for suspension feeders residing there. Finally, these results provide a detailed framework of FA abundances that can be used in trophic and diet studies dedicated to the Subantarctic islands.

F. Acknowledgments

We thank B. Quéguiner, the PI of the MOBYDICK project, for providing us the opportunity to participate to this cruise, the chief scientist I. Obernosterer and the captain and crew of the R/V Marion Dufresne for their enthusiasm and support aboard during the MOBYDICK–THEMISTO cruise (https://doi.org/10.17600/18000403). This work was supported by the French oceanographic fleet ("Flotte océanographique française"), the French ANR ("Agence Nationale de la Recherche", AAPG 2017 program, MOBYDICK Project number: ANR-17-CE01-0013), the French Research program of INSU-CNRS LEFE/CYBER ("Les enveloppes fluides et l'environnement" – "Cycles biogéochimiques, environnement et ressources"). Marine Remize PhD fellowship and studies was supported by the University of Brest (UBO, France), the Center of Marine Sciences (CMS) of the University of North Carolina Wilmington (UNCW, USA), the "Laboratoire d'Excellence" LabexMer (ANR-10-LABX-19), and the Walter-Zellidja grant of the Académie Française. E. Puccinelli was supported by ISblue project, Interdisciplinary graduate school for the blue planet (ANR-17-EURE-0015) and co-funded by a grant from the French government under the program "Investissements d'Avenir". We would like to thank our colleagues of the Technical Division of the INSU, Emmanuel de Saint-Leger, Lionel Scouarnec, Lionel Fischen, and Olivier Desprez De Gesincourt for their logistical and technical help with the in-situ pumps, the colleagues of the UBO Open Factory for their help in designing and preparing the NITEX membranes, and also to Stephane Blain and Bernard Quéguiner for their helpful comments and suggestions on the manuscript.

G. References

Alonso, D.L., Belarbi, E.-H., Rodríguez-Ruiz, J., Segura, C.I., Giménez, A., 1998. Acyl lipids of three microalgae. Phytochemistry 47, 1473–1481. https://doi.org/10.1016/S0031-9422(97)01080-7

Arendt, K.E., Jónasdóttir, S.H., Hansen, P.J., Gärtner, S., 2005. Effects of dietary fatty acids on the reproductive success of the calanoid copepod Temora longicornis. Marine Biology 146, 513–530. https://doi.org/10.1007/s00227-004-1457-9

Armand, L.K., Cornet-Barthaux, V., Mosseri, J., Quéguiner, B., 2008. Late summer diatom biomass and community structure on and around the naturally iron-fertilised Kerguelen Plateau in the Southern Ocean. Deep Sea Research Part II: Topical Studies in Oceanography 55, 653–676. https://doi.org/10.1016/j.dsr2.2007.12.031

Atkinson, A., Shreeve, R.S., Hirst, A.G., Rothery, P., Tarling, G.A., Pond, D.W., Korb, R.E., Murphy, E.J., Watkins, J.L., 2006. Natural growth rates in Antarctic krill (Euphausia superba): II. Predictive models based on food, temperature, body length, sex, and maturity stage. Limnology and Oceanography 51, 973–987. https://doi.org/10.4319/lo.2006.51.2.0973

Bec, A., Martin-Creuzburg, D., von Elert, E., 2006. Trophic upgrading of autotrophic picoplankton by the heterotrophic nanoflagellate Paraphysomonas sp. Limnology and Oceanography 51, 1699–1707. https://doi.org/10.4319/lo.2006.51.4.1699

Blain, S., Queguiner, B., Armand, L., Belviso, S., Bombled, B., Bopp, L., Bowie, A., Brunet, C., Brussaard, C., Carlotti, F., Christaki, U., Corbiere, A., Durand, I., Ebersbach, F., Fuda, J.-L., Garcia, N., Gerringa, L., Griffiths, B., Guigue, C., Guillerm, C., Jacquet, S., Jeandel, C., Laan, P., Lefevre, D., Lo Monaco, C., Malits, A., Mosseri, J., Obernosterer, I., Park, Y.-H., Picheral, M., Pondaven, P., Remenyi, T., Sandroni, V., Sarthou, G., Savoye, N., Scouarnec, L., Souhaut, M., Thuiller, D., Timmermans, K., Trull, T., Uitz, J., van Beek, P., Veldhuis, M., Vincent, D., Viollier, E., Vong, L., Wagener, T., 2007. Effect of natural iron fertilization on carbon sequestration in the Southern Ocean. Nature 446, 1070–1074. https://doi.org/10.1038/nature05700

Blain, S., Rembauville, M., Crispi, O., Obernosterer, I., 2021. Synchronized autonomous sampling reveals coupled pulses of biomass and export of morphologically different diatoms in the Southern Ocean. Limnology and Oceanography 66, 753–764. https://doi.org/10.1002/lno.11638

877 Blain, S., Sarthou, G., Laan, P., 2008. Distribution of dissolved iron during the natural iron-
878 fertilization experiment KEOPS (Kerguelen Plateau, Southern Ocean). Deep Sea Research Part II:
879 Topical Studies in Oceanography 55, 594–605. https://doi.org/10.1016/j.dsr2.2007.12.028

880 Brett, M.T., Müller-Navarra, D., 1997. The role of highly unsaturated fatty acids in aquatic food
881 web processes. Freshwater Biology 38, 483–499. https://doi.org/10.1046/j.1365-2427.1997.00220.x

882 Brett, M.T., Müller-Navarra, D.C., Persson, J., 2009. Crustacean zooplankton fatty acid
883 composition, in: Kainz, M., Brett, M., Arts, M. (Eds.), Lipids in Aquatic Ecosystems. Springer, New
884 York, NY.

885 Broglio, E., Jónasdóttir, S.H., Calbet, A., Jakobsen, H.H., Saiz, E., 2003. Effect of heterotrophic
886 versus autotrophic food on feeding and reproduction of the calanoid copepod Acartia tonsa:
887 relationship with prey fatty acid composition. Aquat Microb Ecol 31, 267–278.

888 Brooks, P.D., Geilmann, H., Werner, R.A., Brand, W., 2003. Improved precision of coupled 13C
889 and 15N measurements from single samples using an elemental analyser. Rapid Communications
890 in Mass Spectrometry 12, 1924–1926. https://doi.org/10.1002/rcm.1134

891 Budge, S.M., Iverson, S.J., Koopman, H.N., 2006. Studying trophic ecology in marine
892 ecosystems using fatty acids: a primer on analysis and interpretation. Marine Mammal Science 22,
893 759–801.

894 Budge, S.M., Parrish, C.C., 1998. Lipid biogeochemistry of plankton, settling matter and
895 sediments in Trinity Bay, Newfoundland. II. Fatty acids. Organic Geochemistry 29, 1547–1559.
896 https://doi.org/10.1016/S0146-6380(98)00177-6

897 Cañavate, J.P., 2019. Advancing assessment of marine phytoplankton community structure
898 and nutritional value from fatty acid profiles of cultured microalgae. Reviews in Aquaculture 11,
899 527–549. https://doi.org/10.1111/raq.12244

900 Cañavate, J.-P., van Bergeijk, S., González-Ortegón, E., Vílas, C., 2021. Contrasting fatty acids
901 with other indicators to assess nutritional status of suspended particulate organic matter in a

902 turbid estuary. Estuarine, Coastal and Shelf Science 254, 107329.
903 https://doi.org/10.1016/j.ecss.2021.107329

904 Cavagna, A.J., Fripiat, F., Elskens, M., Mangion, P., Chirurgien, L., Closset, I., Lasbleiz, M.,
905 Florez-Leiva, L., Cardinal, D., Leblanc, K., Fernandez, C., Lefèvre, D., Oriol, L., Blain, S.,
906 Quéguiner, B., Dehairs, F., 2015. Production regime and associated N cycling in the vicinity of
907 Kerguelen Island, Southern Ocean. Biogeosciences 12, 6515–6528. https://doi.org/10.5194/bg-12-
908 6515-2015

909 Christaki, U., Gueneugues, A., Liu, Y., Blain, S., Catala, P., Colombet, J., Debeljak, P., Jardillier,
910 L., Irion, S., Planchon, F., Sassenhagen, I., Sime-Ngando, T., Obernosterer, I., 2020. Seasonal
911 microbial food web dynamics in contrasting Southern Ocean productivity regimes. Limnology
912 and Oceanography n/a. https://doi.org/10.1002/lno.11591

913 Christaki, U., Skouroliakou, I.-D., Delegrange, A., Irion, S., Courcot, L., Jardillier, L.,
914 Sassenhagen, I., 2021. Microzooplankton diversity and potential role in carbon cycling of
915 contrasting Southern Ocean productivity regimes. Journal of Marine Systems 219, 103531.
916 https://doi.org/10.1016/j.jmarsys.2021.103531

917 Claustre, H., Poulet, S.A., Williams, R., Marty, J.C., Coombs, S., Mlih, F.B., Hapette, A.M.,
918 Jezequel-Martin, V., 1990. A biochemical investigation of a Phaeocystis sp. bloom in the Irish Sea.
919 Journal of the Marine Biological Association of the United Kingdom 70, 197–207.
920 https://doi.org/10.1017/S0025315400034317

921 Constable, A.J., Melbourne-Thomas, J., Corney, S.P., Arrigo, K.R., Barbraud, C., Barnes,
922 D.K.A., Bindoff, N.L., Boyd, P.W., Brandt, A., Costa, D.P., Davidson, A.T., Ducklow, H.W.,
923 Emmerson, L., Fukuchi, M., Gutt, J., Hindell, M.A., Hofmann, E.E., Hosie, G.W., Iida, T., Jacob, S.,
924 Johnston, N.M., Kawaguchi, S., Kokubun, N., Koubbi, P., Lea, M.-A., Makhado, A., Massom, R.A.,
925 Meiners, K., Meredith, M.P., Murphy, E.J., Nicol, S., Reid, K., Richerson, K., Riddle, M.J., Rintoul,
926 S.R., Smith Jr, W.O., Southwell, C., Stark, J.S., Sumner, M., Swadling, K.M., Takahashi, K.T.,
927 Trathan, P.N., Welsford, D.C., Weimerskirch, H., Westwood, K.J., Wienecke, B.C., Wolf-Gladrow,
928 D., Wright, S.W., Xavier, J.C., Ziegler, P., 2014. Climate change and Southern Ocean ecosystems I:

929 how changes in physical habitats directly affect marine biota. Global Change Biology 20, 3004–
930 3025. https://doi.org/10.1111/gcb.12623

931 Conte, M.H., Dickey, T.D., Weber, J.C., Johnson, R.J., Knap, A.H., 2003. Transient physical
932 forcing of pulsed export of bioreactive material to the deep Sargasso Sea. Deep Sea Research Part
933 I: Oceanographic Research Papers 50, 1157–1187. https://doi.org/10.1016/S0967-0637(03)00141-9

934 Conte, M.H., Eglinton, G., Madreira, L.A.S., Rabouille, C., Labeyrie, L., Mudge, S., Eglinton,
935 G., Elderfield, H., Whitfield, M., Williams, P.J.Le.B., 1995. Origin and fate of organic biomarker
936 compounds in the water column and sediments of the eastern North Atlantic. Philosophical
937 Transactions of the Royal Society of London. Series B: Biological Sciences 348, 169–178.
938 https://doi.org/10.1098/rstb.1995.0059

939 Dalsgaard, J., St. John, M., Kattner, G., Müller-Navarra, D., Hagen, W., 2003. Fatty acid trophic
940 markers in the pelagic marine environment, in: Advances in Marine Biology. Academic Press, pp.
941 225–340. https://doi.org/10.1016/S0065-2881(03)46005-7

942 de Baar, H.J.W., de Jong, J.T.M., Bakker, D.C.E., Loscher, B.M., Veth, C., Bathmann, U.,
943 Smetacek, V., 1995. Importance of iron for plankton blooms and carbon dioxide drawdown in the
944 Southern Ocean. Nature 373, 412–415. https://doi.org/10.1038/373412a0

945 Deppeler, S.L., Davidson, A.T., 2017. Southern Ocean Phytoplankton in a Changing Climate.
946 Frontiers in Marine Science 4. https://doi.org/10.3389/fmars.2017.00040

947 Dunstan, G.A., Volkman, J.K., Barrett, S.M., Leroi, J.-M., Jeffrey, S.W., 1993. Essential
948 polyunsaturated fatty acids from 14 species of diatom (Bacillariophyceae). Phytochemistry 35,
949 155–161. https://doi.org/10.1016/S0031-9422(00)90525-9

950 Ebersbach, F., Trull, T.W., 2008. Sinking particle properties from polyacrylamide gels during
951 the KErguelen Ocean and Plateau compared Study (KEOPS): Zooplankton control of carbon
952 export in an area of persistent natural iron inputs in the Southern Ocean. Limnol. Oceanogr. 53,
953 212–224. https://doi.org/10.4319/lo.2008.53.1.0212

954 El-Sayed, S.Z., 1988. Productivity of the southern ocean: a closer look. Comparative
955 Biochemistry and Physiology Part B: Comparative Biochemistry 90, 489–498.
956 https://doi.org/10.1016/0305-0491(88)90287-8

957 Ericson, J.A., Hellessey, N., Nichols, P.D., Kawaguchi, S., Nicol, S., Hoem, N., Virtue, P., 2018.
958 Seasonal and interannual variations in the fatty acid composition of adult Euphausia superba
959 Dana, 1850 (Euphausiacea) samples derived from the Scotia Sea krill fishery. Journal of
960 Crustacean Biology 38, 662–672. https://doi.org/10.1093/jcbiol/ruy032

961 Evans, C., Brussaard, C.P.D., 2012. Viral lysis and microzooplankton grazing of
962 phytoplankton throughout the Southern Ocean. Limnology and Oceanography 57, 1826–1837.
963 https://doi.org/10.4319/lo.2012.57.6.1826

964 Fahl, K., Kattner, G., 1993. Lipid content and fatty acid composition of algal communities in
965 sea-ice and water from the Weddell Sea (Antarctica). Polar Biology 13, 405–409.
966 https://doi.org/10.1007/BF01681982

967 Falk-Petersen, S., Hagen, W., Kattner, G., Clarke, A., Sargent, J., 2000. Lipids, trophic
968 relationships, and biodiversity in Arctic and Antarctic krill. Canadian Journal of Fisheries and
969 Aquatic Sciences 57, 178–191. https://doi.org/10.1139/f00-194

970 Fiala, M., Kopczynska, E.E., Jeandel, C., Oriol, L., Vetion, G., 1998. Seasonal and interannual
971 variability of size-fractionated phytoplankton biomass and community structure at station Kerfix,
972 off the Kerguelen Islands, Antarctica. Journal of Plankton Research 20, 1341–1356.
973 https://doi.org/10.1093/plankt/20.7.1341

974 Gillan, F.T., McFadden, G.I., Wetherbee, R., Johns, R.B., 1981. Sterols and fatty acids of an
975 Antarctic sea ice diatoms, Stauroneis amphioxys. Phytochemistry 20, 1935–1937.

976 Guo, F., Bunn, S.E., Brett, M.T., Kainz, M., 2017. Polyunsaturated fatty acids in stream food
977 webs - high dissimilarity among producers and consumers. Freshwater Biology 62, 1325–1334.
978 https://doi.org/10.1111/fwb.12956

979 Guschina, I.A., Harwood, J.L., 2006. Lipids and lipid metabolism in eukaryotic algae. Progress
980 in Lipid Research 45, 160–186. https://doi.org/10.1016/j.plipres.2006.01.001

981 Hamm, C., Reigstad, M., Riser, C.W., Mühlebach, Anneke, Wassmann, P., 2001. On the trophic
982 fate of Phaeocystis pouchetii. VII. Sterols and fatty acids reveal sedimentation of P. pouchetii-
983 derived organic matter via krill fecal strings. Mar Ecol Prog Ser 209, 55–69.

984 Hayakawa, K., Handa, N., Ikuta, N., Fukuchi, M., 1996. Downward fluxes of fatty acids and
985 hydrocarbons during a phytoplankton bloom in the austral summer in Breid Bay, Antarctica.
986 Organic Geochemistry 24, 511–521. https://doi.org/10.1016/0146-6380(96)00047-2

987 Hellessey, N., Johnson, R., Ericson, J.A., Nichols, P.D., Kawaguchi, S., Nicol, S., Hoem, N.,
988 Virtue, P., 2020. Antarctic Krill Lipid and Fatty acid Content Variability is Associated to Satellite
989 Derived Chlorophyll a and Sea Surface Temperatures. Scientific Reports 10, 6060.
990 https://doi.org/10.1038/s41598-020-62800-7

991 Hernando, M., Schloss, I.R., Almandoz, G.O., Malanga, G., Varela, D.E., De Troch, M., 2018.
992 Combined effects of temperature and salinity on fatty acid content and lipid damage in Antarctic
993 phytoplankton. Journal of Experimental Marine Biology and Ecology 503, 120–128.
994 https://doi.org/10.1016/j.jembe.2018.03.004

995 Hixson, S.M., Arts, M.T., 2016. Climate warming is predicted to reduce omega-3, long-chain,
996 polyunsaturated fatty acid production in phytoplankton. Global Change Biology 22, 2744–2755.
997 https://doi.org/10.1111/gcb.13295

998 Irion, S., Christaki, U., Berthelot, H., L'Helguen, S., Jardillier, L., 2021. Small phytoplankton
999 contribute greatly to CO2-fixation after the diatom bloom in the Southern Ocean. The ISME
1000 Journal. https://doi.org/10.1038/s41396-021-00915-z

1001 Irion, S., Jardillier, L., Sassenhagen, I., Christaki, U., 2020. Marked spatiotemporal variations
1002 in small phytoplankton structure in contrasted waters of the Southern Ocean (Kerguelen area).
1003 Limnology and Oceanography. https://doi.org/10.1002/lno.11555

1004 Iversen, M.H., Pakhomov, E.A., Hunt, B.P.V., van der Jagt, H., Wolf-Gladrow, D., Klaas, C.,
1005 2017. Sinkers or floaters? Contribution from salp pellets to the export flux during a large bloom
1006 event in the Southern Ocean. Deep Sea Research Part II: Topical Studies in Oceanography 138,
1007 116–125. https://doi.org/10.1016/j.dsr2.2016.12.004

1008 Jiang, Y., Chen, F., 2000. Effects of medium glucose concentration and pH on docosahexaenoic
1009 acid content of heterotrophic Crypthecodinium cohnii. Process Biochemistry 35, 1205–1209.
1010 https://doi.org/10.1016/S0032-9592(00)00163-1

1011 Jónasdóttir, S.H., 2019. Fatty Acid Profiles and Production in Marine Phytoplankton. Marine
1012 Drugs 17, 151.

1013 Kabeya, N., Ogino, M., Ushio, H., Haga, Y., Satoh, S., Navarro, J.C., Monroig, Ó., 2021. A
1014 complete enzymatic capacity for biosynthesis of docosahexaenoic acid (DHA, 22 : 6n–3) exists in
1015 the marine Harpacticoida copepod Tigriopus californicus. Open Biology 11, 200402.
1016 https://doi.org/10.1098/rsob.200402

1017 Kattner, G., Hagen, W., 1995. Polar herbivorous copepods – different pathways in lipid
1018 biosynthesis. ICES Journal of Marine Science 52, 329–335. https://doi.org/10.1016/1054-
1019 3139(95)80048-4

1020 Klein-Breteler, W.C.M., Schogt, N., Baas, M., Schouten, S., Kraay, G.W., 1999. Trophic
1021 upgrading of food quality by protozoans enhancing copepod growth: role of essential lipids.
1022 Marine Biology 135, 191–198. https://doi.org/10.1007/s002270050616

1023 Kopczyńska, E.E., Fiala, M., Jeandel, C., 1998. Annual and interannual variability in
1024 phytoplankton at a permanent station off Kerguelen Islands, Southern Ocean. Polar Biology 20,
1025 342–351. https://doi.org/10.1007/s003000050312

1026 Korb, R.E., Whitehouse, M., 2004. Contrasting primary production regimes around South
1027 Georgia, Southern Ocean: large blooms versus high nutrient, low chlorophyll waters. Deep Sea
1028 Research Part I: Oceanographic Research Papers 51, 721–738.
1029 https://doi.org/10.1016/j.dsr.2004.02.006

1030 Lafond, A., Leblanc, K., Legras, J., Cornet, V., Quéguiner, B., 2020. The structure of diatom
1031 communities constrains biogeochemical properties in surface waters of the Southern Ocean
1032 (Kerguelen Plateau). Journal of Marine Systems 212, 103458.
1033 https://doi.org/10.1016/j.jmarsys.2020.103458

1034 Lasbleiz, M., Leblanc, K., Armand, L.K., Christaki, U., Georges, C., Obernosterer, I.,
1035 Quéguiner, B., 2016. Composition of diatom communities and their contribution to plankton
1036 biomass in the naturally iron-fertilized region of Kerguelen in the Southern Ocean. FEMS
1037 Microbiology Ecology 92, fiw171.

1038 Laurenceau-Cornec, E.C., Trull, T.W., Davies, D.M., Bray, S.G., Doran, J., Planchon, F., Carlotti,
1039 F., Jouandet, M.P., Cavagna, A.J., Waite, A.M., Blain, S., 2015. The relative importance of
1040 phytoplankton aggregates and zooplankton fecal pellets to carbon export: insights from free-
1041 drifting sediment trap deployments in naturally iron-fertilised waters near the Kerguelen Plateau.
1042 Biogeosciences 12, 1007–1027. https://doi.org/10.5194/bg-12-1007-2015

1043 Lim, A.S., Jeong, H.J., You, J.H., Park, S.A., 2020. Semi-continuous cultivation of the
1044 mixotrophic dinoflagellate Gymnodinium smaydae, a new promising microalga for omega-3
1045 production. Algae 35, 277–292. https://doi.org/10.4490/algae.2020.35.9.2

1046 Liu, Y., Blain, S., Crispi, O., Rembauville, M., Obernosterer, I., 2020. Seasonal dynamics of
1047 prokaryotes and their associations with diatoms in the Southern Ocean as revealed by an
1048 autonomous sampler. Environmental Microbiology 22, 3968–3984. https://doi.org/10.1111/1462-
1049 2920.15184

1050 Lund, E.D., Chu, F.-L.E., Harvey, E., Adlof, R., 2008. Mechanism(s) of long chain n-3 essential
1051 fatty acid production in two species of heterotrophic protists: Oxyrrhis marina and Gyrodinium
1052 dominans. Marine Biology 155, 23–36. https://doi.org/10.1007/s00227-008-1003-2

1053 Martin, J.H., 1990. Glacial-interglacial CO2 change: The Iron Hypothesis. Paleoceanography 5,
1054 1–13. https://doi.org/10.1029/PA005i001p00001

1055 Martin-Creuzburg, D., von Elert, E., Hoffmann, K.H., 2008. Nutritional constraints at the
1056 cyanobacteria—Daphnia magna interface: The role of sterols. Limnology and Oceanography 53,
1057 456–468. https://doi.org/10.4319/lo.2008.53.2.0456

1058 Mathieu-Resuge, M., Schaal, G., Kraffe, E., Corvaisier, R., Lebeau, O., Lluch-Costa, S.E.,
1059 Salgado García, R.L., Kainz, M.J., Le Grand, F., 2019. Different particle sources in a bivalve species
1060 of a coastal lagoon: evidence from stable isotopes, fatty acids, and compound-specific stable
1061 isotopes. Marine Biology 166, 89–101.

1062 Mayzaud, P., Laureillard, J., Merien, D., Brinis, A., Godard, C., Razouls, S., Labat, J. –P, 2007.
1063 Zooplankton nutrition, storage and fecal lipid composition in different water masses associated
1064 with the Agulhas and Subtropical Fronts. Marine Chemistry 107, 202–213.
1065 https://doi.org/10.1016/j.marchem.2007.07.001

1066 Mayzaud, P., Tirelli, V., Errhif, A., Labat, J.P., Razouls, S., Perissinotto, R., 2002. Carbon intake
1067 by zooplankton. Importance and role of zooplankton grazing in the Indian sector of the Southern
1068 Ocean. Deep Sea Research Part II: Topical Studies in Oceanography 49, 3169–3187.
1069 https://doi.org/10.1016/S0967-0645(02)00077-2

1070 Mitani, E., Nakayama, F., Matsuwaki, I., Ichi, I., Kawabata, A., Kawachi, M., Kato, M., 2017.
1071 Fatty acid composition profiles of 235 strains of three microalgal divisions within the NIES
1072 Microbial Culture Collection. Microb. Resour. Syst 33, 1929.

1073 Moline, M.A., Claustre, H., Frazer, T.K., Schofield, O., Vernet, M., 2004. Alteration of the food
1074 web along the Antarctic Peninsula in response to a regional warming trend. Global Change
1075 Biology 10, 1973–1980. https://doi.org/10.1111/j.1365-2486.2004.00825.x

1076 Mongin, M., Molina, E., Trull, T.W., 2008. Seasonality and scale of the Kerguelen plateau
1077 phytoplankton bloom: A remote sensing and modeling analysis of the influence of natural iron
1078 fertilization in the Southern Ocean. Deep Sea Research Part II: Topical Studies in Oceanography
1079 55, 880–892. https://doi.org/10.1016/j.dsr2.2007.12.039

1080 Monroig, Ó., Kabeya, N., 2018. Desaturases and elongases involved in polyunsaturated fatty
1081 acid biosynthesis in aquatic invertebrates: a comprehensive review. Fisheries Science 84, 911–928.
1082 https://doi.org/10.1007/s12562-018-1254-x

1083 Müller-Navarra, D.C., Brett, M.T., Liston, A.M., Goldman, C.R., 2000. A highly unsaturated
1084 fatty acid predicts carbon transfer between primary producers and consumers. Nature 403, 74–77.
1085 https://doi.org/10.1038/47469

1086 Nichols, D.S., Nichols, P.D., Sullivan, C.W., 1993. Fatty acid, sterol and hydrocarbon
1087 composition of Antarctic sea ice diatom communities during the spring bloom in McMurdo
1088 Sound. Antartic Science 5, 271–278.

1089 Nichols, P.D., Skerratt, J.H., Davidson, A., Burton, H., McMeekin, T.A., 1991. Lipids of
1090 cultured Phaeocystis pouchetii: Signatures for food-web, biogeochemical and environmental
1091 studies in Antarctica and the Southern ocean. Phytochemistry 30, 3209–3214.
1092 https://doi.org/10.1016/0031-9422(91)83177-M

1093 Nielsen, B.L.H., Gøtterup, L., Jørgensen, T.S., Hansen, B.W., Hansen, L.H., Mortensen, J.,
1094 Jepsen, P.M., 2019. n-3 PUFA biosynthesis by the copepod Apocyclops royi documented using
1095 fatty acid profile analysis and gene expression analysis. Biology Open 8.
1096 https://doi.org/10.1242/bio.038331

1097 Okuyama, H., Morita, N., Kogame, K., 1992. Occurrence of octadecapentaenoic acid in lipids
1098 of a cold stenothermic alga, prymnesiophyte strain B. Journal of Phycology 28, 465–472.

1099 Orsi, A.H., Whitworth, T., Nowlin, W.D., 1995. On the meridional extent and fronts of the
1100 Antarctic Circumpolar Current. Deep Sea Research Part I: Oceanographic Research Papers 42,
1101 641–673. https://doi.org/10.1016/0967-0637(95)00021-W

1102 Pakhomov, E.A., McQuaid, C.D., 1996. Distribution of surface zooplankton and seabirds
1103 across the Southern Ocean. Polar Biology 16, 271–286. https://doi.org/10.1007/s003000050054

Park, Y.-H., Fuda, J.-L., Durand, I., Naveira Garabato, A.C., 2008. Internal tides and vertical mixing over the Kerguelen Plateau. Deep Sea Research Part II: Topical Studies in Oceanography 55, 582–593. https://doi.org/10.1016/j.dsr2.2007.12.027

Parrish, C.C., 2013. Lipids in marine ecosystems. ISRN Oceanography 2013, 604045. https://doi.org/10.5402/2013/604045

Pauthenet, E., Roquet, F., Madec, G., Guinet, C., Hindell, M., McMahon, C.R., Harcourt, R., Nerini, D., 2018. Seasonal Meandering of the Polar Front Upstream of the Kerguelen Plateau. Geophysical Research Letters 45, 9774–9781. https://doi.org/10.1029/2018gl079614

Pellichero, V., Boutin, J., Claustre, H., Merlivat, L., Sallée, J.-B., Blain, S., 2020. Relaxation of Wind Stress Drives the Abrupt Onset of Biological Carbon Uptake in the Kerguelen Bloom: A Multisensor Approach. Geophysical Research Letters 47, e2019GL085992. https://doi.org/10.1029/2019gl085992

Perissinotto, R., Duncombe Rae, C.M., 1990. Occurrence of anticyclonic eddies on the Prince Edward Plateau (Southern Ocean): effects on phytoplankton biomass and production. Deep Sea Research Part A. Oceanographic Research Papers 37, 777–793. https://doi.org/10.1016/0198-0149(90)90006-H

Pollard, R., Sanders, R., Lucas, M., Statham, P., 2007. The Crozet Natural Iron Bloom and Export Experiment (CROZEX). Deep Sea Research Part II: Topical Studies in Oceanography 54, 1905–1914. https://doi.org/10.1016/j.dsr2.2007.07.023

Pond, D.W., Atkinson, A., Shreeve, R.S., Tarling, G., Ward, P., 2005. Diatom fatty acid biomarkers indicate recent growth rates in Antarctic krill. Limnology and Oceanography 50, 732–736. https://doi.org/10.4319/lo.2005.50.2.0732

Quéroué, F., Sarthou, G., Planquette, H.F., Bucciarelli, E., Chever, F., van der Merwe, P., Lannuzel, D., Townsend, A.T., Cheize, M., Blain, S., d'Ovidio, F., Bowie, A.R., 2015. High variability of dissolved iron concentrations in the vicinity of Kerguelen Island (Southern Ocean). Biogeosciences Discuss. 12, 231–270. https://doi.org/10.5194/bgd-12-231-2015

1130 Rembauville, M., Blain, S., Armand, L., Quéguiner, B., Salter, I., 2015a. Export fluxes in a
1131 naturally iron-fertilized area of the Southern Ocean – Part 2: Importance of diatom resting spores
1132 and faecal pellets for export. Biogeosciences 12, 3171–3195. https://doi.org/10.5194/bg-12-3171-
1133 2015

1134 Rembauville, M., Blain, S., Manno, C., Tarling, G., Thompson, A., Wolff, G., Salter, I., 2018.
1135 The role of diatom resting spores in pelagic–benthic coupling in the Southern Ocean.
1136 Biogeosciences 15, 3071–3084. https://doi.org/10.5194/bg-15-3071-2018

1137 Rembauville, M., Salter, I., Dehairs, F., Miquel, J.-C., Blain, S., 2017. Annual particulate matter
1138 and diatom export in a high nutrient, low chlorophyll area of the Southern Ocean. Polar Biology.
1139 https://doi.org/10.1007/s00300-017-2167-3

1140 Rembauville, M., Salter, I., Leblond, N., Gueneugues, A., Blain, S., 2015b. Export fluxes in a
1141 naturally iron-fertilized area of the Southern Ocean – Part 1: Seasonal dynamics of particulate
1142 organic carbon export from a moored sediment trap. Biogeosciences 12, 3153–3170.
1143 https://doi.org/10.5194/bg-12-3153-2015

1144 Remize, M., Planchon, F., Loh, A.N., Le Grand, F., Bideau, A., Le Goic, N., Fleury, E., Miner,
1145 P., Corvaisier, R., Volety, A., Soudant, P., 2020. Study of Synthesis Pathways of the Essential
1146 Polyunsaturated Fatty Acid 20:5n-3 in the Diatom Chaetoceros Muelleri Using 13C-Isotope
1147 Labeling. Biomolecules 10. https://doi.org/10.3390/biom10050797

1148 Salter, I., Kemp, A.E.S., Moore, C.M., Lampitt, R.S., Wolff, G.A., Holtvoeth, J., 2012. Diatom
1149 resting spore ecology drives enhanced carbon export from a naturally iron-fertilized bloom in the
1150 Southern Ocean. Global Biogeochemical Cycles 26, GB1014. https://doi.org/10.1029/2010gb003977

1151 Salter, I., Lampitt, R.S., Sanders, R., Poulton, A., Kemp, A.E.S., Boorman, B., Saw, K., Pearce,
1152 R., 2007. Estimating carbon, silica and diatom export from a naturally fertilised phytoplankton
1153 bloom in the Southern Ocean using PELAGRA: A novel drifting sediment trap. Deep Sea Research
1154 Part II: Topical Studies in Oceanography 54, 2233–2259. https://doi.org/10.1016/j.dsr2.2007.06.008

1155 Sargent, J.R., Eilertsen, H.C., Falk-Petersen, S., Taasen, J.P., 1985. Carbon assimilation and lipid
1156 production in phytoplankton in northern Norwegian fjords. Marine Biology 85, 109–116.
1157 https://doi.org/10.1007/BF00397428

1158 Sassenhagen, I., Irion, S., Jardillier, L., Moreira, D., Christaki, U., 2020. Protist Interactions and
1159 Community Structure During Early Autumn in the Kerguelen Region (Southern Ocean). Protist
1160 171, 125709. https://doi.org/10.1016/j.protis.2019.125709

1161 Schallenberg, C., Bestley, S., Klocker, A., Trull, T.W., Davies, D.M., Gault-Ringold, M., Eriksen,
1162 R., Roden, N.P., Sander, S.G., Sumner, M., Townsend, A.T., van der Merwe, P., Westwood, K.,
1163 Wuttig, K., Bowie, A., 2018. Sustained Upwelling of Subsurface Iron Supplies Seasonally
1164 Persistent Phytoplankton Blooms Around the Southern Kerguelen Plateau, Southern Ocean.
1165 Journal of Geophysical Research: Oceans 123, 5986–6003. https://doi.org/10.1029/2018jc013932

1166 Schlosser, C., Schmidt, K., Aquilina, A., Homoky, W.B., Castrillejo, M., Mills, R.A., Patey,
1167 M.D., Fielding, S., Atkinson, A., Achterberg, E.P., 2018. Mechanisms of dissolved and labile
1168 particulate iron supply to shelf waters and phytoplankton blooms off South Georgia, Southern
1169 Ocean. Biogeosciences 15, 4973–4993. https://doi.org/10.5194/bg-15-4973-2018

1170 Seeyave, S., Lucas, M.I., Moore, C.M., Poulton, A.J., 2007. Phytoplankton productivity and
1171 community structure in the vicinity of the Crozet Plateau during austral summer 2004/2005. Deep
1172 Sea Research Part II: Topical Studies in Oceanography 54, 2020–2044.
1173 https://doi.org/10.1016/j.dsr2.2007.06.010

1174 Sheridan, C.C., Lee, C., Wakeham, S.G., Bishop, J.K.B., 2002. Suspended particle organic
1175 composition and cycling in surface and midwaters of the equatorial Pacific Ocean. Deep Sea
1176 Research Part I: Oceanographic Research Papers 49, 1983–2008. https://doi.org/10.1016/S0967-
1177 0637(02)00118-8

1178 Skerratt, J.H., Nichols, P.D., McMeekin, T.A., Burton, H., 1995. Seasonal and inter-annual
1179 changes in planktonic biomass and community structure in eastern Antarctica using signature
1180 lipids. Marine Chemistry 51, 93–113. https://doi.org/10.1016/0304-4203(95)00047-U

1181 Tang, K.W., Jakobsen, H.H., Visser, A.W., 2001. Phaeocystis globosa (Prymnesiophyceae) and
1182 the planktonic food web: Feeding, growth, and trophic interactions among grazers. Limnology
1183 and Oceanography 46, 1860–1870. https://doi.org/10.4319/lo.2001.46.8.1860

1184 Thomson, P.G., Wright, S.W., Bolch, C.J.S., Nichols, P.D., Skerratt, J.H., McMinn, A., 2004.
1185 Antarctic distribution, pigment and lipid composition, and molecular identification of the brine
1186 dinoflagellate Polarella glacialis (Dinophycae). Journal of Phycology 40, 867–873.
1187 https://doi.org/10.1111/j.1529-8817.2004.03169.x

1188 Trull, T.W., Davies, D.M., Dehairs, F., Cavagna, A.J., Lasbleiz, M., Laurenceau-Cornec, E.C.,
1189 d'Ovidio, F., Planchon, F., Leblanc, K., Quéguiner, B., Blain, S., 2015. Chemometric perspectives
1190 on plankton community responses to natural iron fertilisation over and downstream of the
1191 Kerguelen Plateau in the Southern Ocean. Biogeosciences 12, 1029–1056.
1192 https://doi.org/10.5194/bg-12-1029-2015

1193 Vaezi, R., Napier, J.A., Sayanova, O., 2013. Identification and functional characterization of
1194 genes encoding omega-3 polyunsaturated fatty acid biosynthetic activities from unicellular
1195 microalgae. Marine drugs 11, 5116–5129.

1196 van der Merwe, P., Bowie, A.R., Quéroué, F., Armand, L., Blain, S., Chever, F., Davies, D.,
1197 Dehairs, F., Planchon, F., Sarthou, G., Townsend, A.T., Trull, T.W., 2015. Sourcing the iron in the
1198 naturally fertilised bloom around the Kerguelen Plateau: particulate trace metal dynamics.
1199 Biogeosciences 12, 739–755. https://doi.org/10.5194/bg-12-739-2015

1200 Venables, H., Moore, C.M., 2010. Phytoplankton and light limitation in the Southern Ocean:
1201 Learning from high-nutrient, high-chlorophyll areas. Journal of Geophysical Research: Oceans
1202 115. https://doi.org/10.1029/2009jc005361

1203 Virtue, P., Nichols, P.D., Nicol, S., McMinn, A., Sikes, E.L., 1993. The lipid composition of
1204 Euphausia superba Dana in relation to the nutritional value of Phaeocystis pouchetii (Hariot)
1205 Lagerheim. Antarctic Science 5, 169–177. https://doi.org/10.1017/S0954102093000239

1206 Volkman, J.K., Barrett, S.M., Blackburn, S.I., Mansour, M.P., Sikes, E.L., Gelin, F., 1998.
1207 Microalgal biomarkers: A review of recent research developments. Organic Chemistry 29, 1163–
1208 1179. https://doi.org/10.1016/S0146-6380(98)00062-X

1209 Wakeham, S.G., 1995. Lipid biomarkers for heterotrophic alteration of suspended particulate
1210 organic matter in oxygenated and anoxic water columns of the ocean. Deep Sea Research Part I:
1211 Oceanographic Research Papers 42, 1749–1771. https://doi.org/10.1016/0967-0637(95)00074-G

1212 Wang, S.W., Budge, S.M., Iken, K., Gradinger, R.R., Springer, A.M., Wooller, M.J., 2015.
1213 Importance of sympagic production to Bering Sea zooplankton as revealed from fatty acid-carbon
1214 stable isotope analyses. Mar Ecol Prog Ser 518, 31–50.

1215 Wilson, S.E., Steinberg, D.K., Chu, F.L.E., Bishop, J.K.B., 2010. Feeding ecology of mesopelagic
1216 zooplankton of the subtropical and subarctic North Pacific Ocean determined with fatty acid
1217 biomarkers. Deep Sea Research Part I: Oceanographic Research Papers 57, 1278–1294.
1218 https://doi.org/10.1016/j.dsr.2010.07.005

1219